Received: 3 January 2020 | Revised: 7 September 2020 | Accepted: 9 September 2020

DOI: 10.1111/cmi.13263

RESEARCH ARTICLE

WILEY

SopB- and SifA-dependent shaping of the *Salmonella*-containing vacuole proteome in the social amoeba *Dictyostelium discoideum*

Camila Valenzuela[1,2,3] | Magdalena Gil[2,3] | Ítalo M. Urrutia[1] | Andrea Sabag[1] | Jost Enninga[2,3] | Carlos A. Santiviago[1]

[1]Laboratorio de Microbiología, Departamento de Bioquímica y Biología Molecular, Facultad de Ciencias Químicas y Farmacéuticas, Universidad de Chile, Santiago, Chile

[2]Dynamics of Host-Pathogen Interactions Unit, Institut Pasteur, Paris, France

[3]CNRS UMR3691, Paris, France

Correspondence
Carlos A. Santiviago, Laboratorio de Microbiología, Departamento de Bioquímica y Biología Molecular, Facultad de Ciencias Químicas y Farmacéuticas, Universidad de Chile, Santiago, Chile.
Email: csantiviago@ciq.uchile.cl

Funding information
Comisión Nacional de Investigación Científica y Tecnológica (CONICYT), fellowships, Grant/Award Numbers: 21140615, 21150005; Fondo Nacional de Desarrollo Científico y Tecnológico (FONDECYT), grants, Grant/Award Numbers: 1140754, 1171844

Abstract

The ability of *Salmonella* to survive and replicate within mammalian host cells involves the generation of a membranous compartment known as the *Salmonella*-containing vacuole (SCV). *Salmonella* employs a number of effector proteins that are injected into host cells for SCV formation using its type-3 secretion systems encoded in SPI-1 and SPI-2 (T3SS-1 and T3SS-2, respectively). Recently, we reported that *S.* Typhimurium requires T3SS-1 and T3SS-2 to survive in the model amoeba *Dictyostelium discoideum*. Despite these findings, the involved effector proteins have not been identified yet. Therefore, we evaluated the role of two major *S.* Typhimurium effectors SopB and SifA during *D. discoideum* intracellular niche formation. First, we established that *S.* Typhimurium resides in a vacuolar compartment within *D. discoideum*. Next, we isolated SCVs from amoebae infected with wild type or the Δ*sopB* and Δ*sifA* mutant strains of *S.* Typhimurium, and we characterised the composition of this compartment by quantitative proteomics. This comparative analysis suggests that *S.* Typhimurium requires SopB and SifA to modify the SCV proteome in order to generate a suitable intracellular niche in *D. discoideum*. Accordingly, we observed that SopB and SifA are needed for intracellular survival of *S.* Typhimurium in this organism. Thus, our results provide insight into the mechanisms employed by *Salmonella* to survive intracellularly in phagocytic amoebae.

KEYWORDS
Dictyostelium, intracellular survival, proteome, *Salmonella*, SCV, T3SS

1 | INTRODUCTION

Bacteria from the *Salmonella* genus infect warm-blooded animals targeting the gastrointestinal tract. Particular serovars, such as *Salmonella enterica* serovar Typhimurium (*S.* Typhimurium), represent major leading causes of gastroenteritis in humans in developing countries (World Health Organization, 2015). Overall, *Salmonella* infections account for over 150,000 deaths annually in the world, most of them associated with foodborne infections (World Health Organization, 2015).

Among the genes required for *Salmonella* virulence, pathogenicity islands SPI-1 and SPI-2 encode two independent type-3 secretion systems (T3SS). These systems are macromolecular structures used to inject effector proteins directly into targeted host cells, and they play major roles during successive steps of the infection cycle. The T3SS encoded in SPI-1 (T3SS-1) and its cognate effectors are required during the intestinal phase of the infection, allowing the invasion of epithelial cells through the reorganisation of the actin cytoskeleton at the

Camila Valenzuela and Magdalena Gil contributed equally to this work.

bacterial–host contact sites inducing bacterial endocytosis by these nonphagocytic cells (Hardt et al., 1998; Patel & Galán, 2006). In addition, after crossing the epithelial barrier, *Salmonella* may use the T3SS-1 to enter into phagocytic cells residing in the subepithelium, such as macrophages, neutrophils and dendritic cells. The T3SS encoded in SPI-2 (T3SS-2) is expressed upon internalisation within different host cell types. This system and its cognate effectors enable *Salmonella* to avoid phagosome-lysosome fusion and to generate the *Salmonella*-containing vacuole (SCV). Within this membrane-bound compartment, the pathogen can survive and replicate (Cirillo et al., 1998; Hensel et al., 1997; Maskell & Mastroeni, 2006; Rappl et al., 2003; Waterman & Holden, 2003).

One understudied aspect of *Salmonella* biology is its survival in the environment, where the pathogen spends an important part of its life cycle. In this niche, *Salmonella* is exposed to predation by protozoa such as amoebae. These eukaryotic microorganisms are phagocytic cells that feed on bacteria. Multiple studies have demonstrated that different *Salmonella* serovars are able to survive within a number of protozoa genera, such as *Acanthamoeba*, *Tetramitus*, *Naegleria*, *Hartmannella* and *Tetrahymena* (Bleasdale et al., 2009; Brandl et al., 2005; Feng et al., 2009; Gaze et al., 2003; Rehfuss et al., 2011; Tezcan-Merdol et al., 2004; Wildschutte & Lawrence, 2007; Wildschutte et al., 2004). In the case of other intracellular pathogens, such as *Legionella pneumophila*, the mechanisms to survive and replicate inside amoebae have been studied in some detail (Steiner et al., 2018; Swart et al., 2018). Moreover, as in the case of *Salmonella*, *L. pneumophila* injects effector proteins to subvert physiological processes in the host cell in order to survive within amoebae and human macrophages (Gao et al., 1997; Segal & Shuman, 1999). This suggests that the molecular weapons used by intracellular bacterial pathogens have evolved through early interactions with environmental phagocytic organisms. Thus, understanding the mechanisms used by *Salmonella* to survive intracellularly in amoebae will provide insights into how these bacteria acquired the ability to colonise and survive within phagocytic cells, including the macrophages of a given animal host.

Recently, we started characterising the interaction of *Salmonella* with the social amoeba *Dictyostelium discoideum* as this organism has proven to be a powerful model to study host–pathogen interaction for several bacterial pathogens (Cardenal-Muñoz et al., 2017; Müller-Taubenberger et al., 2013; Swart et al., 2018; Taylor-Mulneix et al., 2017). Early reports from different groups presented some discrepancies regarding the use of *D. discoideum* as an appropriate host model for *Salmonella* (Sillo et al., 2011; Skriwan et al., 2002). However, we and other authors have recently described that *S.* Typhimurium is able to survive intracellularly (and proliferate at later times of infection) in *D. discoideum*, and that inactivation of genes encoding relevant virulence factors in other models (including T3SS-1 and T3SS-2) generates defects in intracellular survival in this organism (Frederiksen & Leisner, 2015; Riquelme et al., 2016; Urrutia et al., 2018; Varas et al., 2018). These observations support the use of *D. discoideum* as a suitable model to study the processes involved in the intracellular survival of *S.* Typhimurium.

Effectors such as SopB (secreted by T3SS-1) and SifA (secreted by T3SS-2) have been characterised for their abilities in modifying the SCV composition. In fact, both proteins are major effectors involved in the biogenesis and maturation of the SCV in eukaryotic cells (Ramos-Morales, 2012). SopB is a phosphatidylinositol phosphatase involved in reducing the levels of $PI(4,5)P_2$ in the nascent SCV and in modifying the repertoire of proteins that interact with this compartment, in particular Rab5 and its cognate PI3K, Vps34 (Hernandez et al., 2004; Mallo et al., 2008). Furthermore, SopB is involved in the recruitment of Rab7 resulting in the accumulation of LAMP1, vATPase and other late endosome markers at the SCV (Drecktrah et al., 2007; Garcia-del Portillo & Finlay, 1995; Méresse et al., 1999; Oh et al., 1996). On the other hand, SifA is involved in the maintenance of the SCV membrane integrity by its interaction with other *Salmonella* effectors (Ohlson et al., 2008). SifA also interacts with the molecular motor kinesin using SKIP as an adapter protein. This interaction is crucial to allow the formation of a network of tubular structures known as the *Salmonella*-induced filaments (SIFs) (Diacovich et al., 2009; Dumont et al., 2010).

In this study, we established that *S.* Typhimurium resides in a vacuolar compartment within *D. discoideum*. SCVs isolated from amoebae infected with wild type (WT) and mutant strains of *S.* Typhimurium were subjected to quantitative proteomics to characterise the composition of this compartment. Comparative analysis of the data suggests that effectors SopB and SifA are involved in the modification of the SCV proteome to ensure a suitable niche for *S.* Typhimurium within *D. discoideum*. Consistently, we established that *S.* Typhimurium requires both SopB and SifA to survive intracellularly in this organism. Overall, our results contribute to understanding the mechanisms used by *Salmonella* to survive predation by phagocytic amoebae that may act as reservoirs for this pathogen in the environment.

2 | RESULTS

2.1 | *S.* Typhimurium resides in a vacuolar compartment within infected *D. discoideum*

We evaluated the presence of a vacuolar compartment containing *S.* Typhimurium in *D. discoideum*. For this purpose, infection assays were performed using a reporter *D. discoideum* strain expressing the VatM subunit of the vacuolar ATPase fused to GFP (VatM-GFP). This allowed the visualisation of $VatM^+$ vacuolar compartments by confocal microscopy. Of note, VatM has been shown to be present at the membrane of different vacuolar compartments in *D. discoideum*, including phagosomes, endosomes, lysosomes and the contractile vacuole (Clarke et al., 2002), and the vacuolar ATPase is one of the protein complexes recruited to the SCV in other cellular models (Steele-Mortimer et al., 1999). For our experiments, we used a WT strain of *S.* Typhimurium constitutively expressing fluorescent mCherry (Figueira et al., 2013). We observed that most infected amoebae presented $VatM^+$ structures surrounding intracellular bacteria at different times post infection. Representative images of infected amoebae with the typical VatM-GFP staining in the surrounding of red fluorescent bacteria obtained at 3 and 4.5 hr post infection are shown in Figure S1a

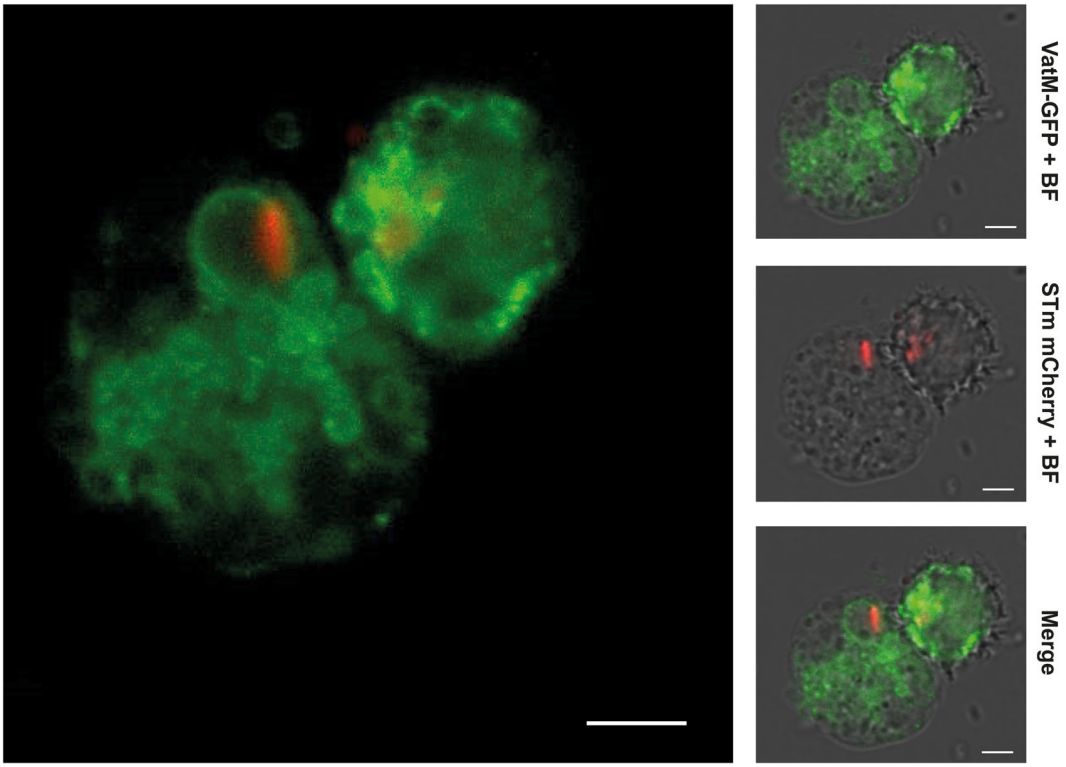

FIGURE 1 *S*. Typhimurium resides in a spacious vacuolar compartment surrounded by the vacuolar ATPase. *S*. Typhimurium 14028s constitutively expressing mCherry was used to infect the axenic strain *D*. *discoideum* AX2 VatM-GFP. Images were acquired at 4.5 hr post infection with a Zeiss LSM 710 confocal microscope using ZEN 2012 Black software (Zeiss) and edited using FIJI software. The green fluorescence corresponds to the fusion protein VatM-GFP, and the red fluorescence corresponds to bacteria expressing mCherry. BF, brightfield. Bar is 2 μm

and Figure 1, respectively. We quantified the colocalisation between $VatM^+$ vacuoles and *S*. Typhimurium and observed that 93% of the intracellular bacteria in infected amoebae are surrounded by the VatM-GFP signal (Figure S1b). These observations confirm the existence of a $VatM^+$ vacuolar compartment containing *S*. Typhimurium within infected *D*. *discoideum*.

2.2 | SopB and SifA effectors are required for intracellular survival of *S*. Typhimurium in *D. discoideum*

Considering that T3SS effectors are crucial for SCV generation in other cellular models, we decided to evaluate the role of two major effectors involved in this process: SopB and SifA. First, we evaluated the intracellular survival of Δ*sifA* and Δ*sopB* mutants of *S*. Typhimurium in *D*. *discoideum*. We anticipated that these mutants would be contained in a vacuolar compartment unable to support the intracellular survival of the pathogen. Therefore, we performed infection assays in *D*. *discoideum* under conditions that have been described by our group (Riquelme et al., 2016; Urrutia et al., 2018) (Figure 2). We found that the number of internalised bacteria was similar between the different strains (Figure 2a), indicating that the deletion of genes *sopB* and *sifA* does not affect the uptake of *S*. Typhimurium by *D. discoideum*. Then, we evaluated the intracellular survival of these strains and observed that the Δ*sifA* mutant presented defects at 3 hr post infection, and that this phenotype became more prominent at 6 hr post infection (Figure 2c). Similarly, the Δ*sopB* mutant also presented growth defects at 6 hr post infection (Figure 2c). The phenotype shown by each mutant was reverted by the presence of a derivative of plasmid pBAD-TOPO harbouring a WT copy of the corresponding gene. No strain significantly changed the number of viable amoebae during the course of the experiment (Figure 2b), indicating that the differences observed in the titers of intracellular Δ*sopB* and Δ*sifA* mutants are not attributable to changes in the number of viable amoebae.

Thus, our results indicate that SopB and SifA effectors are required for the intracellular survival of *S*. Typhimurium in *D*. *discoideum*. Therefore, we decided to examine if the survival defect shown by Δ*sopB* and Δ*sifA* mutants correlates with altered recruitment of host factors to the SCV using a proteomic approach.

2.3 | Preparation of intact SCVs from *D. discoideum* infected with *S*. Typhimurium

To characterise the protein content of the SCV in *D*. *discoideum*, we adapted a protocol originally developed to obtain a subcellular

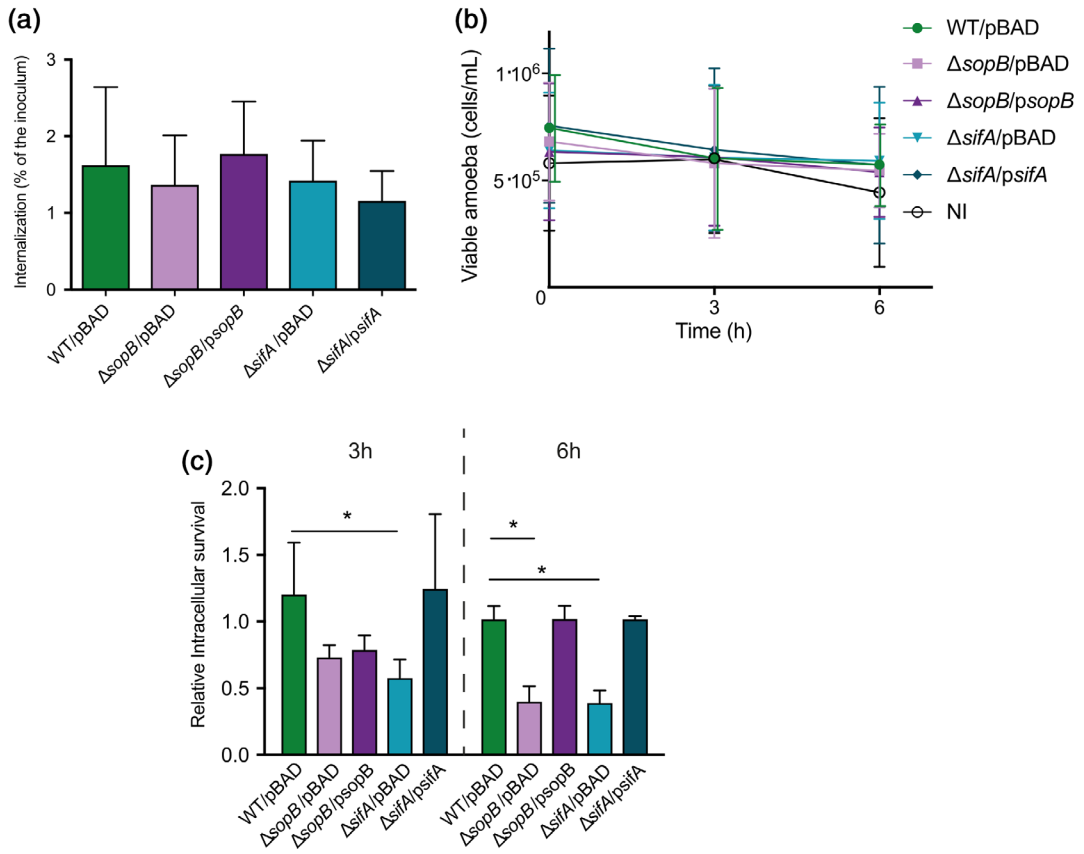

FIGURE 2 Intracellular survival of WT, Δ*sopB* and Δ*sifA* strains of *S.* Typhimurium in *D. discoideum*. (a) Internalisation expressed as the percentage of intracellular bacteria at *t* = 0 relative to the initial inoculum. Statistical significance was determined using a one-way ANOVA. (b) Population of viable amoebae at each time post infection. Statistical significance was determined using a one-way ANOVA. (c) Intracellular survival expressed as CFU/cell at *t* = 3 hr or *t* = 6 hr divided by the CFU/cell at *t* = 0. Statistical significance was determined using a two-way ANOVA with Dunnet's test (* = $P < 0.05$). All graphs show mean values ± SEM of at least three independent assays. NI, not infected

fraction highly enriched in intact SCVs from infected HeLa cells (Santos et al., 2015). To this end, we performed infection assays using our WT strain of *S.* Typhimurium. As described in the Figure S2, infected and uninfected control amoebae were lysed, and the post-nuclear supernatants (PNS) obtained were loaded on top of linear 10–25% Optiprep gradients. After centrifugation, 12 fractions obtained from each sample were analysed. Importantly, PNS from control samples were spiked with a known number of bacteria to determine the migration of non-vacuolarised bacteria in the density gradients. As shown in Figure 3, in control samples, non-vacuolarised bacteria accumulated in fractions F8 and F9 (1.12–1.13 g/cm^3), while in samples from infected amoebae, we noted a shift in this distribution with bacteria also accumulating at the lower-density fractions F6 and F7 (1.09–1.10 g/cm^3). The presence of this differential bacterial distribution between infected and control samples is consistent with previously obtained data of bacteria residing inside vacuoles in infected human cells (Santos et al., 2015). To confirm the presence of vacuoles containing bacteria in our preparations, we performed an anti-*Salmonella* ELISA-based assay (Santos et al., 2015). In this assay, an immobilised anti-*Salmonella* antibody was used to capture free bacteria present in each fraction that were subsequently quantified using a biotin-conjugated anti-*Salmonella* antibody. The samples were then analysed before and after an osmotic shock treatment to break the SCV and release all bacteria residing in this compartment. This procedure provided information on the respective fractions of vacuolar-bound *Salmonella* and free *Salmonella*. As shown in Figure S3, the amount of *Salmonella* detected by our assay in fractions F6 to F8 from infected cells increased after the osmotic shock, while there was no increase in the number of *Salmonella* detected in the lower density fraction before and after the osmotic shock treatment in the case of control samples. In addition, we repeated the infection and fractionation experiments using the *D. discoideum* VatM-GFP reporter strain to evaluate the presence of VatM$^+$ vacuoles and *Salmonella* in the fractions of interest. As depicted in Figure S4, we detected an accumulation of VatM-GFP and *Salmonella* in fractions F6, F7 and F8 from infected cells. However, in control samples, *Salmonella* accumulated preferentially in fractions F9 and F10, while VatM-GFP was detected mainly in fractions F4 to F10. Together, these results indicate that fractions F6 and F7 were enriched in intact VatM$^+$ vacuoles containing *Salmonella*. Consequently, we used this fractionation procedure to analyse the protein composition of the SCV.

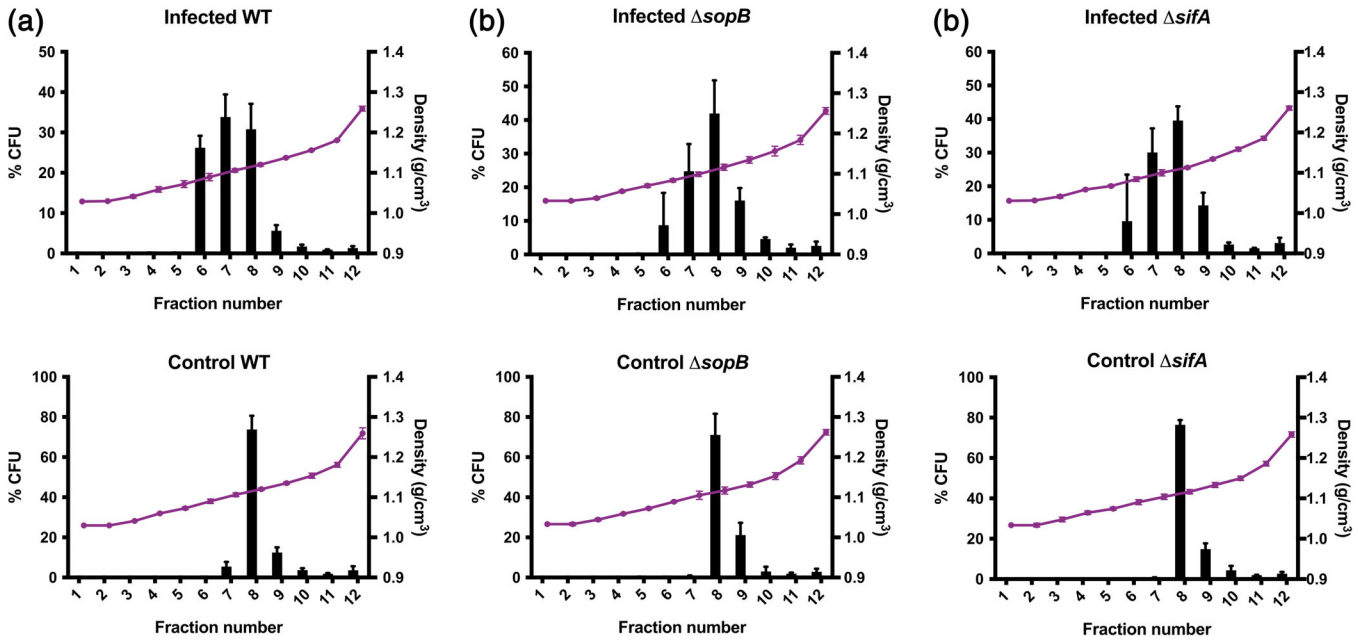

FIGURE 3 Subcellular fractionation of *D. discoideum* cells infected with *S.* Typhimurium strains and uninfected control cells. Graphs show the CFU distribution and Optiprep density per fraction of PNS samples obtained from cells infected with (a) *S.* Typhimurium WT, (b) Δ*sopB* or (b) Δ*sifA*, respectively (upper panels) or PNS from uninfected control cells spiked with a known amount of the same *S.* Typhimurium strain (lower panels). Each graph shows mean values ± *SD* from at least three independent experiments

Additionally, we wanted to evaluate the impact of the absence of effectors SopB and SifA on the proteome of the SCV in *D. discoideum*. To this end, we performed the infection assays and fractionation experiments using our Δ*sopB* and Δ*sifA* mutant strains. In this case, we also observed the shift in bacterial distribution between control and infected samples (Figure 3), although the increase of bacteria in F6 was not as evident as in samples from amoebae infected with the WT strain. When these samples were analysed by our anti-*Salmonella* ELISA, we observed an increase in *Salmonella* detected after the osmotic rupture of the vacuoles (Figure S3), indicating the presence of intact vacuoles containing the *Salmonella* strains in the samples obtained from infected cells. For each bacterial strain infecting *D. discoideum*, four biological replicates were obtained for proteomic analyses.

2.4 | Proteomic analysis of SCVs recovered from infected *D. discoideum*

Fractions F6 and F7 from each experiment were selected for proteomic analysis. These fractions were subjected to protein precipitation, and the proteins from both fractions per experiment were pooled and analysed by LC–MS/MS. Proteomic data analysis was performed using the PatternLab for Proteomics 4.0 software (Carvalho et al., 2016). We first analysed the data obtained from amoebae infected with the WT strain (WT-infected samples) and the corresponding uninfected control samples. For WT-infected samples 945 proteins were identified, while for control samples 1,011 proteins were identified. After manual curation of these two datasets to remove proteins corresponding to contaminants and some bacterial proteins detected, we identified 714 proteins that were shared between both conditions, 218 proteins present only in WT-infected samples, and 194 proteins present only in uninfected control samples (Figure 4a). Among the proteins present only in WT-infected samples, we found proteins related to intracellular trafficking (TrappC2l, TrappC4, RdiA, DDB_G0268048, DymB, GacN, RacD, RipA, GacO,Rab32C, GefQ and GefP); proteins involved in multivesicular body formation (Chmp3 and Chmp6); motor proteins (Kif13, DynC1li1 and Kif5) and actin-related proteins (ForB, ArpA and Act22), among others. The complete list of proteins present exclusively in WT-infected samples is presented in Table S1. Next, we analysed the proteins common to WT-infected and control samples to evaluate their differential distribution and pinpoint those that were enriched in samples obtained from infected cells, according to their normalised spectral abundance factors (NSAF). To do this, we used the PatternLab TFold module to generate a volcano plot according to the fold change (F-change) and *P*-value of each protein (Figure 4b). Light blue dots (NC in Table S2) represent proteins that do not satisfy neither F-change nor statistic criteria and thus were considered as unchanged between both conditions. Teal dots (NSC in Table S2) satisfy the F-change criterion but not the statistical one. Light purple dots (C in Table S2) correspond to low abundant proteins satisfying both the F-change and *Q*-value criteria, but due to the low number of spectra, they deserve further validation. Finally, dark purple dots (SC in Table S2) correspond to proteins satisfying all statistical filters and represent the over- and under-represented proteins between infected

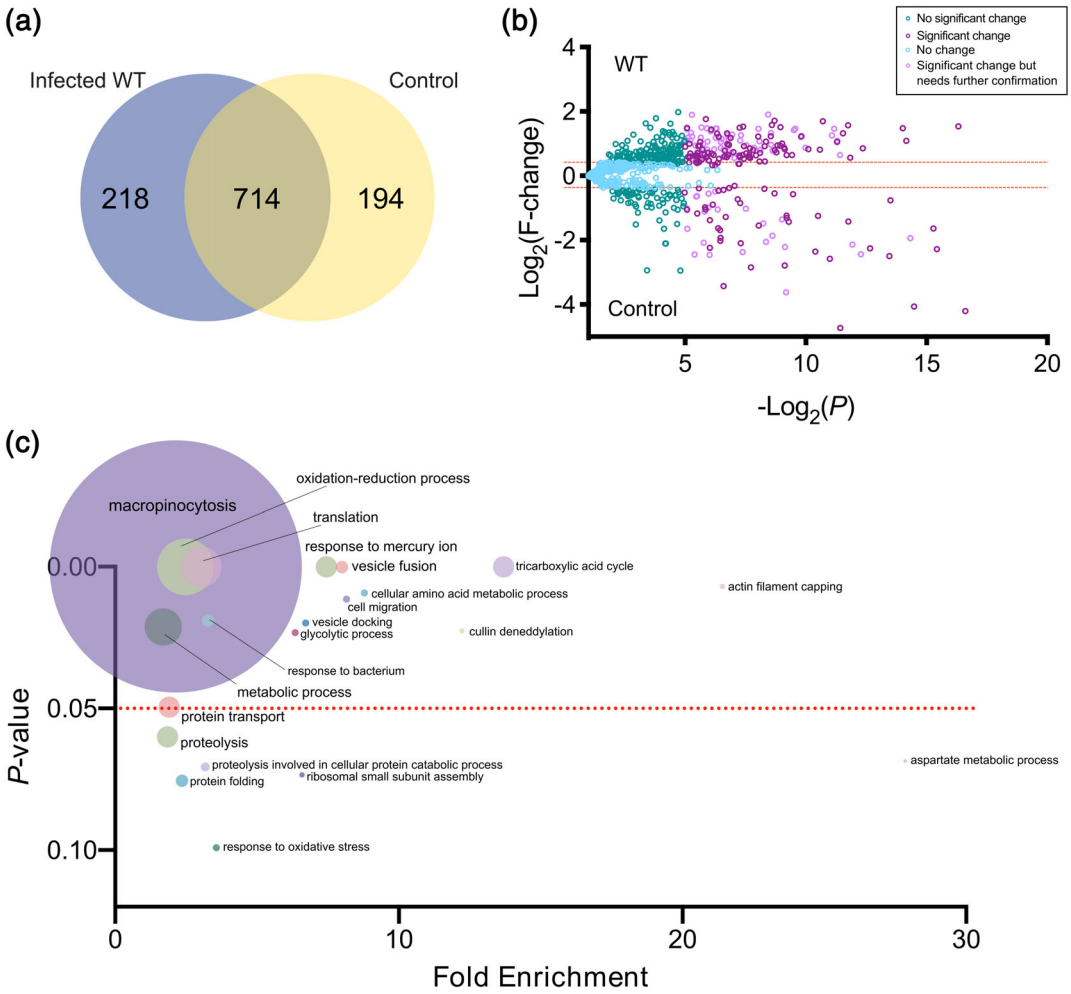

FIGURE 4 Proteomic analysis of WT-infected and uninfected control samples. (a) Venn diagram showing the distribution of proteins identified in samples from cells infected with the WT strain or uninfected control samples. (b) Volcano plot generated using the PatternLab for Proteomics TFold module (FDR of 0.05, F-stringency of 0.03 and *Q*-value of 0.05). For this particular dataset, when a protein presented an F-change >1.25 and a *P*-value <0.05, it was considered to be enriched, and when it presented an F-change < −1.24 and a *P*-value <0.05, it was defined as underrepresented in WT-infected samples. Each dot represents a protein identified in three replicates of all conditions, plotted according to its *P*-value ($Log_2(P)$) and fold change (Log_2(F-change)). (c) Gene ontology functional clustering analysis using DAVID, showing the biological processes enriched in infected samples. Dot size represents the number of proteins enriched in that biological process. All data on these figures can be found in Tables S1 and S2

and control samples. We determined the number of proteins specifically enriched in WT-infected samples: 90 proteins in the SC category and 62 in the C category. Among them, we found trafficking-related proteins (DDB_G0282229, Vti1A, Syn7B, Syn8A, DDB_G0275057 and TrappC5); GTPases (RacE) and actin-related proteins (AcpA, AcpB and ArpC), among others. In addition, we found some proteins related to degradative compartments such as cathepsin D, LmpB (lysosome membrane protein 2-B) and the autophagy marker protein Atg8 (also known as LC3). The complete list of proteins differentially represented between WT-infected and control samples is presented in Table S2.

Next, we analysed the data from Δ*sopB*- and Δ*sifA*-infected samples using the same parameters used for the comparison of control and WT-infected samples. In the case of the Δ*sopB*-infected samples 1,164 proteins were identified, while 1,011 proteins were identified in the control samples. Among all proteins detected, 779 were shared between both experimental conditions, 368 were present only in Δ*sopB*-infected samples, and 129 were present only in control samples (Figure S5a,b, Tables S3 & S4). In the case of the Δ*sifA*-infected samples, 1,088 proteins were identified, whereas 1,011 proteins were identified in the control samples. Among all proteins detected, we identified 746 that were shared between both experimental conditions, 323 present only in Δ*sifA*-infected samples, and 162 present only in control samples (Figure S5c,d, Tables S5 & S6).

To directly compare the data from samples from amoebae infected with either Δ*sopB* or Δ*sifA* mutants with data from WT-infected samples, we used a slightly different approach. Briefly, we compared three datasets (WT-infected, control and Δ*sifA*- or Δ*sopB*-infected cells) and removed all the proteins that are shared between WT-infected and control samples and between Δ*sifA*- or Δ*sopB*-

infected and control samples, along with those proteins exclusively present in the control dataset. This allowed us to directly compare the proteome of SCVs containing the WT strain with that of SCVs containing Δ*sifA* or Δ*sopB* mutant.

In the case of the Δ*sopB*-infected samples, 368 proteins were identified, while 218 proteins were identified in the corresponding WT-infected samples. The comparison of these two datasets (Figure 5a) showed 163 proteins shared between both experimental conditions, 205 proteins present only in Δ*sopB*-infected samples (Table S7) and 55 proteins present only in WT-infected samples (Table S8). Among the proteins detected exclusively in Δ*sopB*-infected samples, we found proteins related to intracellular trafficking; components of the exocyst complex (ExoC3, ExoC5, ExoC6 and ExoC7); Ras guanine nucleotide exchange factors (GEFs) and Rho GTPase-activating proteins (GAPs) (GefE, GacI, GacM, GacN and GacO); motor proteins; ubiquitin and SUMO conjugation enzymes (Pex4 and Ubc9); several serine/threonine kinases and autophagy-related proteins Atg5 and Atg12, among others. The complete list of proteins exclusively present in Δ*sopB*-infected samples is presented in Table S7. We also determined that 14 proteins in the SC category and 2 in the C category were specifically enriched in Δ*sopB*-infected samples when comparing with the WT-infected samples (Figure 5b). Among the proteins specifically enriched in Δ*sopB*-infected samples, we found those related to regulation of small GTPases (GacN and GacO) and proteins of the proteasome complex. The complete list of proteins differentially represented between Δ*sopB*-infected and WT-infected samples is presented in Table S9.

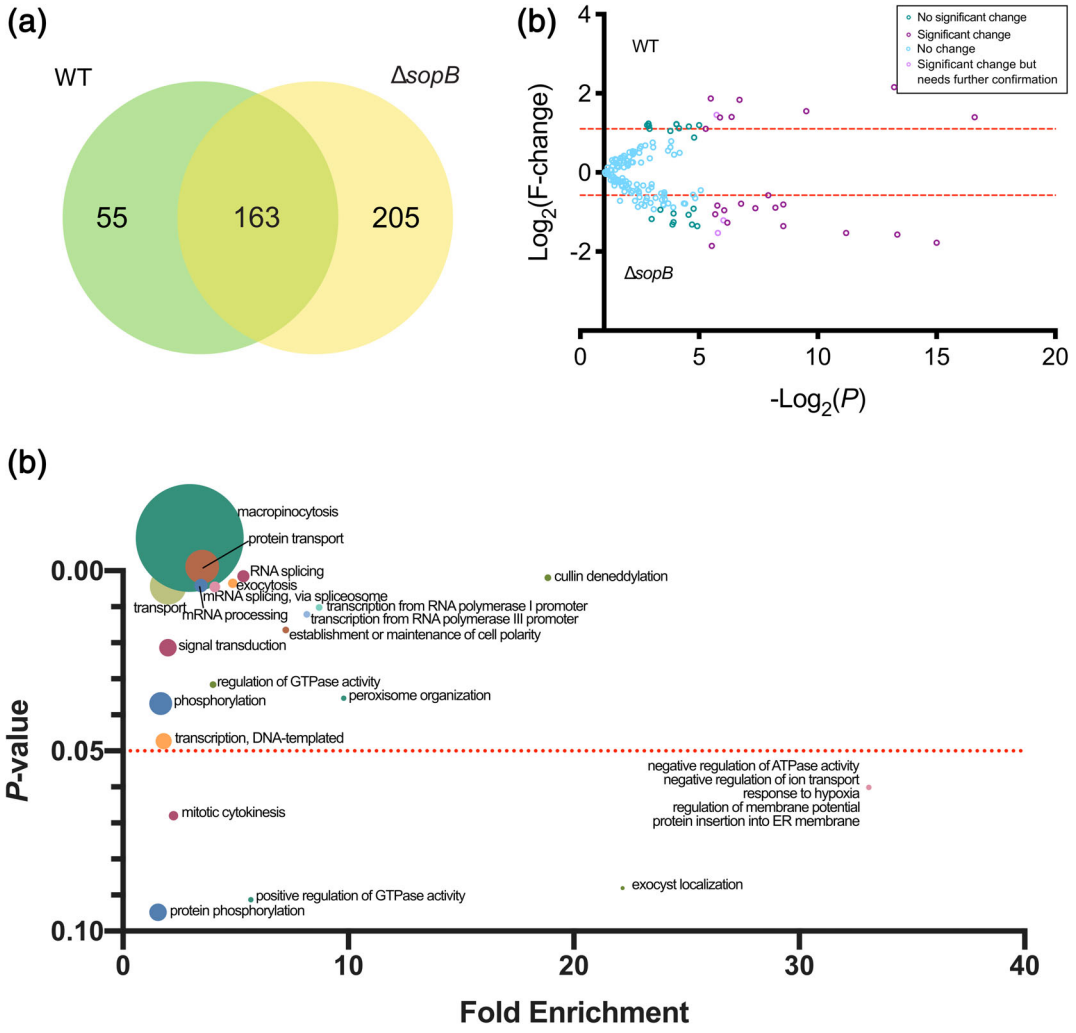

FIGURE 5 Proteomic analysis of Δ*sopB*-infected and WT-infected samples. (a) Venn diagram showing the distribution of proteins identified in samples from cells infected with the Δ*sopB* mutant or uninfected control samples. (b) Volcano plot generated using the PatternLab for Proteomics TFold module (FDR of 0.05, F-stringency of 0.08 and *Q*-value of 0.05). For this comparison, when a protein presented an F-change >2.15 and a *P*-value < 0.05, it was considered to be enriched and when it presented an F-change < −1.49 and a *P*-value < 0.05, it was defined as underrepresented in Δ*sopB*-infected samples. Each dot represents a protein identified in four replicates of all conditions, plotted according to its *P*-value ($Log_2(P)$) and fold change (Log_2(F-change)). (b) Gene ontology functional clustering analysis using DAVID, showing the biological processes enriched in infected samples. Dot size represents the number of proteins enriched in that biological process. All data on these figures can be found in Tables S7, S8, and S9

In the case of the Δ*sifA*-infected samples, 323 proteins were identified, while 218 proteins were identified in the corresponding WT-infected samples. By comparing these two datasets (Figure 6a), we identified 159 proteins shared between both experimental conditions, 164 proteins present only in Δ*sifA*-infected samples (Table S10), and 59 proteins present only in WT-infected samples (Table S11). Among the proteins present exclusively in Δ*sifA*-infected samples, we found the autophagy-related proteins Atg3, Atg5 and Atg12; ubiquitin and SUMO conjugation enzymes; GAPs and GEFs (GpgA, GacI, GacJ, GacM, GacP, DDB_G0281809 and GefE); proteins related to the COP9 signalosome (Csn1, Csn2, Csn3, Csn5, Csn6 and Csn7); proteasome complex proteins (PsmE3, PsmA6 and PsmA3); exocyst complex proteins (ExoC1, ExoC3 and ExoC5) and cathepsin B (CtsB), among others. The complete list of proteins that are present exclusively in Δ*sifA*-infected samples is presented in Table S10. Using the TFold module to analyse the distribution between proteins in these two conditions, we determined that 11 proteins in the SC category and 2 in the C category were specifically enriched in Δ*sifA*-infected samples (Figure 6b). In this group, we found proteins related to the same pathways of those present exclusively in Δ*sopB*-infected samples, such as trafficking proteins and proteasome complex proteins (PsmA3 and PsmA6). The complete list of proteins differentially represented between Δ*sifA*-infected and WT-infected samples is presented in Table S12.

In addition to the analyses described above, we performed a functional clustering analysis using database for annotation, visualization and integrated discovery (DAVID) (Huang et al., 2009a, 2009b) for all the proteins identified only in samples infected with a particular *Salmonella* strain plus those enriched in samples from that experimental condition. The overview of the biological processes associated with

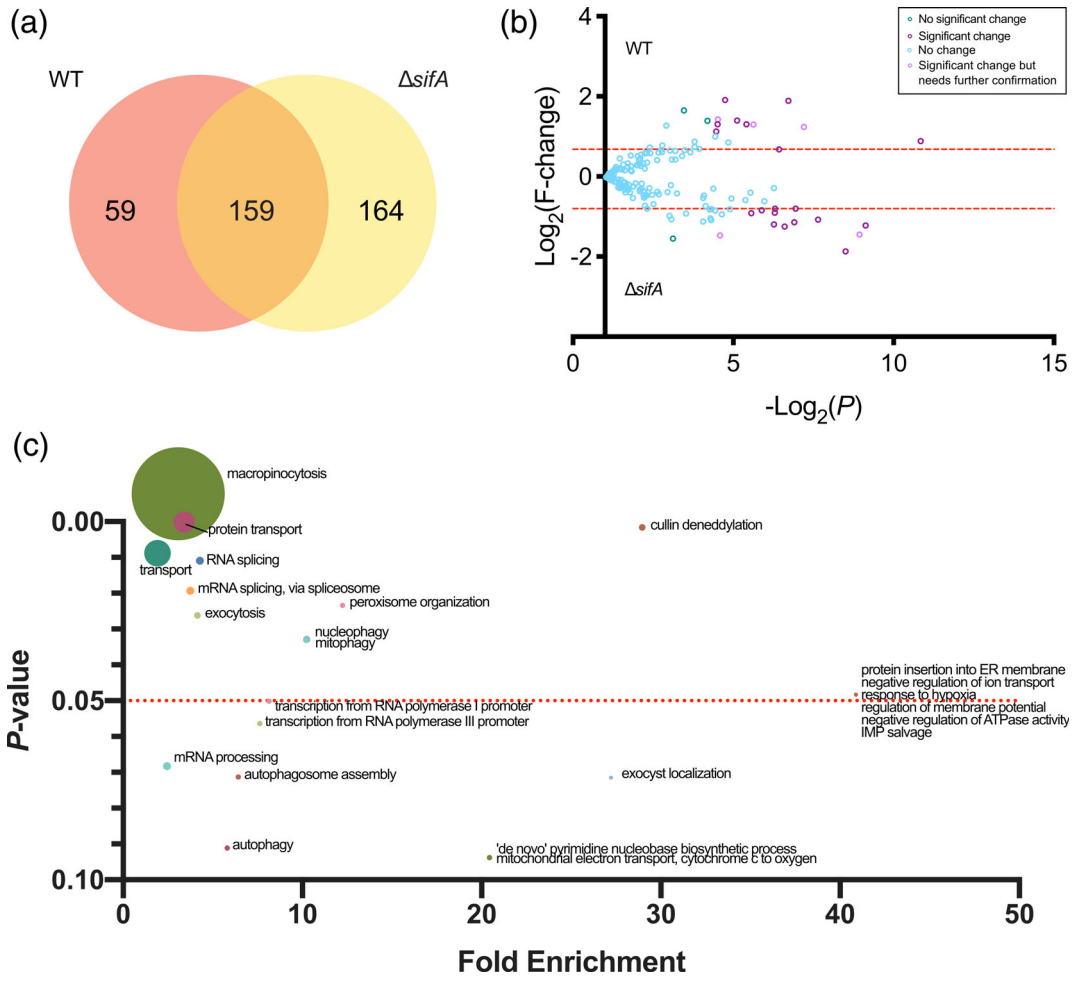

FIGURE 6 Proteomic analysis of Δ*sifA*-infected and WT-infected samples. (**a**) Venn Diagram showing the distribution of proteins identified in samples from cells infected with the Δ*sifA* mutant or uninfected control samples. (**b**) Volcano plot generated using the PatternLab for Proteomics TFold module (FDR of 0.05, F-stringency of 0.23 and *Q*-value of 0.05). For this dataset, when a protein presented an F-change >1.60 and a *P*-value < 0.05, it was considered to be enriched, and when it presented an F-change < −1.75 and a *P*-value < 0.05, it was considered as underrepresented in Δ*sifA*-infected samples. Each dot represents a protein identified in four replicates of all conditions, plotted according to its *P*-value ($Log_2(P)$) and fold change (Log_2(F-change)). (**c**) Gene ontology functional clustering analysis using DAVID, showing the biological processes enriched in infected samples. Dot size represents the number of proteins enriched in that biological process. All data on these figures can be found in Tables S10, S11, and S12

proteins detected in each experimental condition is shown in Figures 4c, 5c, and 6c. In all cases, most proteins appeared as groups related to specific cellular processes such as intracellular trafficking, macropinocytosis and autophagy.

Overall, our fractionation procedure followed by quantitative proteomics allowed us to characterise the SCV composition during *D. discoideum* infections with *S.* Typhimurium. Furthermore, differences in SCV proteomes from amoebae infected with WT, Δ*sopB* and Δ*sifA* strains suggest that the effectors SopB and SifA are required to generate a mature vacuolar compartment that escapes from degradative pathways and sustains the intracellular lifestyle of the pathogen in this host.

2.5 | Autophagy proteins are recruited to the SCV

Since we detected the presence of proteins related to autophagy in the SCV proteome of the analysed samples, we decided to validate this observation. We used GFP-tagged versions of Atg9 (involved in autophagy initiation) (Stanley et al., 2014; Xiong et al., 2015) and Atg16 (involved in the elongation of membranes associated to autophagosomes) (Tung et al., 2010; Xiong et al., 2015) to evaluate the presence of autophagy machinery associated to the SCV during *S.* Typhimurium infection of *D. discoideum* by confocal microscopy. Our results showed that Atg9 and Atg16 colocalised with intracellular *S.* Typhimurium in *D. discoideum* at 3 hr post infection (Figure 7), validating the presence of autophagy proteins in our proteomic analysis. These observations suggest that membranous structures containing autophagy proteins contact the SCV, thus highlighting the importance of this physiological process in the interaction between *S.* Typhimurium and *D. discoideum*.

3 | DISCUSSION

3.1 | *S.* Typhimurium resides in a vacuolar compartment in *D. discoideum*

In the present study, we first analysed the presence of a vacuolar compartment that contained *S.* Typhimurium in infected *D. discoideum*

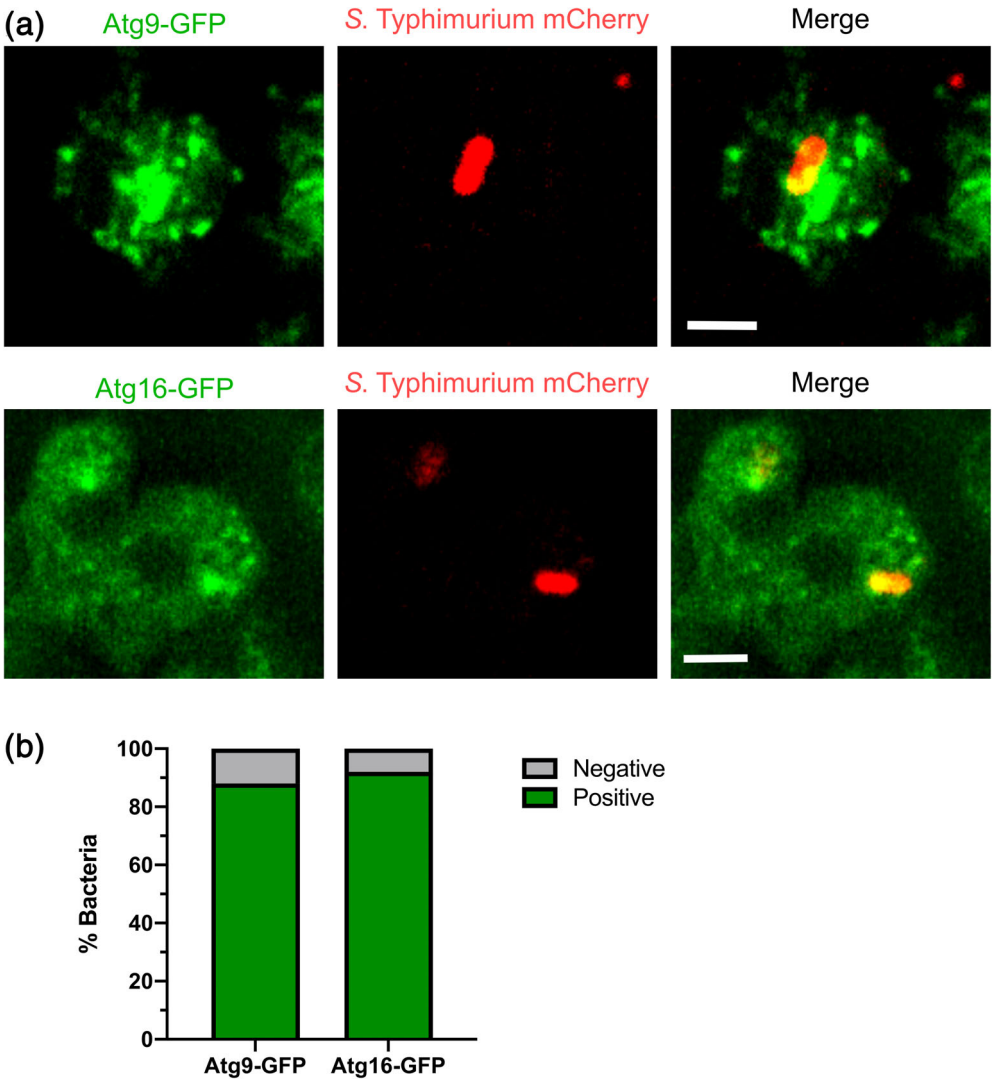

FIGURE 7 Autophagy proteins are associated with the SCV in *D. discoideum*. (a) *S.* Typhimurium 14028s constitutively expressing mCherry was used to infect the axenic strains *D. discoideum* AX2 Atg9-GFP or Atg16-GFP. Images were acquired at 3 hr post infection. The green fluorescence corresponds to GFP-tagged proteins, and the red fluorescence corresponds to bacteria expressing mCherry. Bar is 4 μm. (b) Quantitative analysis of colocalisation between intracellular *S.* Typhimurium and Atg9-GFP or Atg16-GFP in *D. discoideum*

cells. To evaluate the presence of such compartment, we employed confocal microscopy and performed bacterial infections using a *D. discoideum* reporter strain that expresses a component of the vATPase called VatM fused to GFP. This enzyme uses ATP hydrolysis to transport protons across membranes and is composed of two subcomplexes: V_1 and V_0 (Clarke et al., 2002). VatM is part of the V_0 complex and has been localised to the membranes of the contractile vacuole in *D. discoideum* (Heuser et al., 1993); and in membranes of the endolysosomal system (Adessi et al., 1995), in which vATPase acidifies the lumen of endosomes. Furthermore, the vATPase is also present in the SCV in HeLa and macrophage cells (Drecktrah et al., 2007; Knuff & Finlay, 2017; Steele-Mortimer, 2008; Steele-Mortimer et al., 1999). In our experiments, we observed the presence of the VatM-GFP marker in vacuoles containing *S.* Typhimurium at 3 and 4.5 hr post infection. This confirmed that *S.* Typhimurium is contained in a vacuolar compartment in *D. discoideum*, as described by other groups (Skriwan et al., 2002), and that this compartment is a $VatM^+$ vacuole. Other pathogens such as *Mycobacterium marinum* and *Legionella pneumophila* also reside within a membrane-bound compartment in *D. discoideum* (Cardenal-Muñoz et al., 2017; Weber et al., 2018). Of note, in the case of *M. marinum*, there is a selective exclusion of the vATPase from the *Mycobacterium*-containing vacuole (MCV) to avoid acidification of the vacuole (Koliwer-Brandl et al., 2019) and in the case of *L. pneumophila*, VatA (another vATPase subunit) is also excluded from the *Legionella*-containing vacuole (LCV) (Peracino et al., 2010).

3.2 | *S.* Typhimurium requires effectors SopB and SifA to survive intracellularly in *D. discoideum*

The role of the effector proteins SopB and SifA in the intracellular survival of *Salmonella* in other hosts has been widely reported. *In vitro*, it has been shown that SopB contributes to invasion of HeLa cells (Mallo et al., 2008) but is dispensable for intracellular replication in intestinal Henle-407 cells (Hernandez et al., 2004). On the other hand, this effector is required for intracellular growth of *Salmonella* in bone marrow–derived macrophages (Hernandez et al., 2004), which is similar to the phenotype we observe in *D. discoideum*. *SopB* also plays a critical role in the size control of the SCV and its stability (Stévenin et al., 2019). In the case of SifA, it has been shown that *sifA* mutants are strongly attenuated in mice (Holden et al., 2002), but they show a higher percentage of escape from the SCV and hyperreplicate in the cytosol of HeLa cells (Brumell et al., 2002). In addition, *sifA* mutants are defective for intracellular replication in restrictive cell lines such as Swiss 3 T3 fibroblasts and RAW 264.7 macrophages (Holden et al., 2002). Hyperreplication of *Salmonella* has not been described in *D. discoideum*, and we have no evidence of this particular phenotype in this model. Moreover, it has been shown that *Salmonella* requires SopB and SifA to survive and grow intracellularly in mammalian phagocytic cells (Hernandez et al., 2004; Holden et al., 2002). Consistent with these phenotypes, our results show that both effectors play a critical role in the intracellular survival of *S.* Typhimurium in *D. discoideum*.

3.3 | The proteome of the vacuolar compartment containing *S.* Typhimurium in *D. discoideum*

The SCV has been predominantly characterised in infected HeLa cells, and the proteome of the compartment in this cell line has been reported (Santos et al., 2015). This study identified about 400 proteins, and the data showed a significant enrichment in proteins from several organelles, including ER, early and late endosomes, trans-Golgi network and lysosomes, along with vesicle-transport-related proteins and cytoskeleton proteins that may act stabilising SIFs. *Salmonella* replication in these cells is highly permissive, in contrast to replication in macrophages and other phagocytic cells. For this reason, our analysis of the compartment containing *Salmonella* in *D. discoideum* could be more comparable to studies performed in macrophages and to other bacteria-containing compartments in phagocytic cells. Only recently, the isolation of SCVs from human THP-1 macrophages using paramagnetic nanoparticles attached to the surface of *S.* Typhimurium has been reported (Singh et al., 2018). The study performed an initial characterisation of classical SCV-associated proteins, such as Rab5 and LAMP-1, but did not analyse the proteome of this vesicular compartment. Furthermore, the nanoparticles attached to the bacterial surface may influence the internalisation pathway, which alters the initial compartment formed and influences how *S.* Typhimurium subverts the host trafficking pathways (Fredlund et al., 2018).

In a related study in *L. pneumophila*, the proteomes of LCVs from *D. discoideum* and RAW264.7 macrophages were compared (Hoffmann et al., 2014). This highlighted the similarities between both compartments in the two host cells. In this study, numerous LCV proteins identified from infected RAW264.7 macrophages have been described in the literature, including several small GTPases (Urwyler et al., 2009). When compared to proteins identified in LCVs from *D. discoideum*, the authors found a considerable number of proteins implicated in the same signalling pathways, including Ser/Thr and Tyr protein kinases and phosphatases, cyclin-dependent kinases, small GTPases of the Rho/Rac, Ras or Ran families, GTPase modulators, ubiquitin-dependent factors, multivesicular body (MVB) proteins, cargo receptors, dynamin-like GTPases, sorting nexins (SNXs), syntaxins, motor proteins (dynein, kinesin and myosin) and factors implicated in microtubule dynamics (Hoffmann et al., 2014). Interestingly, our proteome results are similar regarding the type of SCV proteins identified and the biological processes involved, as we found SNARE proteins, motor proteins, ubiquitin ligases, Ser/Thr kinases and phosphatases, and MVB proteins, among others. In contrast, our results differ particularly in the Rab GTPases that are enriched in the LCV proteome, as we found that these proteins are not enriched in SCV proteomes. These differences are likely due to the activity of specific effectors secreted by the different bacteria that generate distinct pathogen-specific niches.

In the SCV proteomes obtained from *D. discoideum* infected with the mutant strains, we found several proteins involved in degradative pathways, such as ubiquitin ligases, COP9 signalosome (a type of proteasome that cleaves ubiquitin conjugates and ubiquitin-like protein conjugates, among other targets) (Rosel & Kimmel, 2006; Wei et al., 2008) and autophagy-related proteins. Autophagy is a highly conserved process from yeast to mammals, and many genes associated with autophagy (*atg*) are conserved in amoebae, plants, worms and mammals, emphasising the importance of this process. Autophagy also controls infections caused by intracellular pathogens, as they can be captured in autophagosomes for degradation. In *D. discoideum*, autophagy is the main process that allows this organism to fight intracellular pathogens that escape the endolysosomal degradation pathway (Calvo-Garrido et al., 2010; Dunn et al., 2018). Pathogens such as *M. marinum* have been described to subvert autophagy in *D. discoideum* by inducing the autophagy pathway via transient inhibition of TORC1 activity at early stages of interaction and avoiding being killed inside autolysosomes by blocking the autophagic flux (Cardenal-Muñoz et al., 2017). This results in the accumulation of membranes and cytoplasmic material in the MCV, which might support bacterial survival within this niche.

Similar mechanisms have been described in *Salmonella*, as ruptured SCVs are recognised by galectins (cytoplasmic lectins that bind specific carbohydrate modifications within the ruptured SCV), which subsequently recruit adaptors and autophagosomes (Thurston et al., 2012). Moreover, several reports indicate that autophagy targets cytoplasmic *Salmonella* for degradation (Thurston et al., 2012; Thurston et al., 2009; Zheng et al., 2009). However, other studies demonstrated a role of the autophagy machinery in the repair of damaged SCV membranes caused by T3SS-1 activity (Kreibich et al., 2015) and that the autophagy machinery associates with cytosolic *Salmonella* and promotes intracellular replication (Yu et al., 2014). Current studies by our group show that *S.* Typhimurium subverts the autophagy machinery in both *D. discoideum* and RAW264.7 macrophages by means of effector proteins secreted by T3SS-1. Yet, another study determined that autophagy is necessary to avoid intracellular replication of *S.* Typhimurium in *D. discoideum*, as amoebae carrying null mutations in genes linked to the autophagy pathway infected with *S.* Typhimurium show a decrease in lifespan and an increased bacterial intracellular replication (Jia et al., 2009). Taking these studies together, our proteomic analysis highlights the importance of the autophagic machinery in the fate of the vacuolar compartment involved in *S.* Typhimurium survival in *D. discoideum*. Additionally, we detected the presence of Atg9 and Atg16 in the vicinity of the WT SCV in *D. discoideum* by confocal microscopy, highlighting the importance of autophagy in the interaction between *S.* Typhimurium and this host. Furthermore, these results suggest that *S.* Typhimurium subverts the autophagy machinery in order to survive within *D. discoideum*. This hypothesis is currently being elucidated by our group.

From our work, we propose a model (Figure 8) in which *Salmonella* is internalised by *D. discoideum* and resides in a specialised vacuolar compartment to avoid phagosome degradation by exploiting the activity of specific effectors secreted through T3SS-1 and T3SS-2. For instance, our results suggest that effectors SopB and SifA contribute to the modification of this vacuole by subverting autophagy and excluding proteins related to other degradative pathways, thus allowing the survival of *S.* Typhimurium within *D. discoideum* and its replication at later times of infection (Urrutia et al., 2018). Altogether, our results indicate that the SCV in *D. discoideum* presents similarities with other pathogen-containing vacuoles, both in this model host and in other phagocytic cells such as macrophages. This highlights the importance of *D. discoideum* as a model to study *Salmonella* survival in phagocytic amoebae. In the future, the data generated in this work can be further explored as a starting point to determine other cellular and bacterial proteins involved in biological processes related to the interaction of *S.* Typhimurium with *D. discoideum*.

4 | EXPERIMENTAL PROCEDURES

4.1 | Bacterial strains and growth conditions

The bacterial strains used in the present study are listed in Table S13. All *S.* Typhimurium strains are derivatives of the WT virulent strain 14028s (Fields et al., 1986). Bacteria were routinely grown in Luria-Bertani (LB) medium (10 g/L tryptone, 5 g/L yeast extract, 5 g/L NaCl) at 37°C with aeration. LB medium was supplemented with ampicillin (Amp; 100 mg/L) or kanamycin (Kan; 75 mg/L) as appropriate. Media were solidified by the addition of agar (15 g/L). All procedures involving the use of pathogenic organisms were conducted following the guidelines in the Biosafety Manual of the National Commission of Scientific and Technological Research (CONICYT) and were approved by the Institutional Biosafety Committee of Universidad de Chile, Campus Norte.

4.2 | Construction of mutant strains, cloning and complementation

S. Typhimurium mutants with specific deletions of *sopB* and *sifA* genes and the concomitant insertion of a Kan-resistance cassette were constructed using the Lambda Red recombination method (Datsenko & Wanner, 2000) with modifications (Santiviago et al., 2009). PCR amplification of the resistance cassette present in plasmid pCLF4 (GenBank accession number EU629214) was carried out under standard conditions using primers listed in Table S14. *S.* Typhimurium strain 14028s carrying plasmid pKD46, which encodes the Red recombinase system, was grown to an OD_{600nm} of 0.5–0.6 at 30°C in LB medium containing Amp and L-arabinose (10 mM). Bacteria were made electrocompetent by sequential washes with ice-cold sterile 10% glycerol and transformed with ~500 ng of each purified PCR product. Transformants were selected at 37°C on LB agar containing Kan. The presence of each mutation was confirmed by PCR amplification using primers flanking the sites of substitution (Table S14). Finally, each mutation was transferred to the WT background by

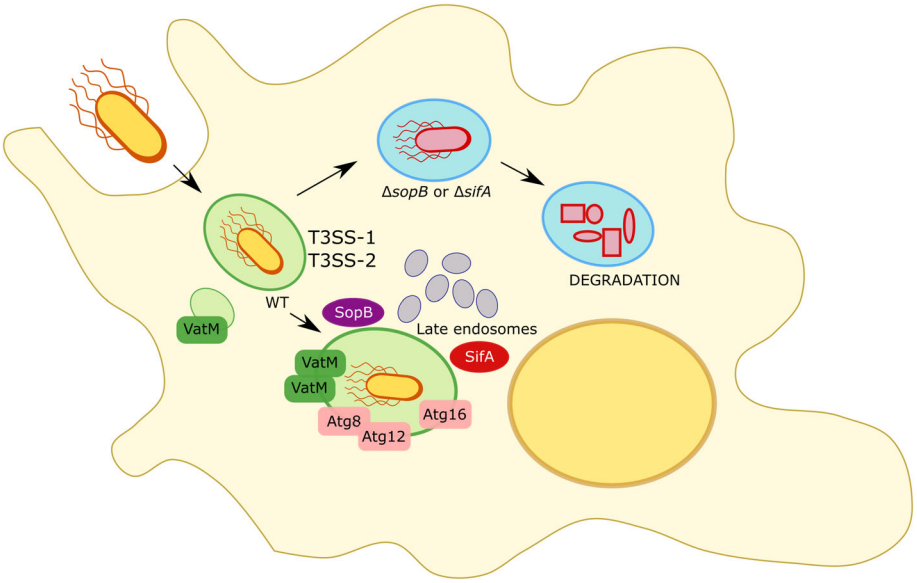

FIGURE 8 Model for the biogenesis of the SCV in *Dictyostelium discoideum*. After internalisation of *Salmonella* by *D. discoideum*, the pathogen resides in a specialised vacuolar compartment that avoids phagosome degradation by exploiting the activity of the effectors SopB and SifA. These proteins subvert autophagy and exclude proteins linked to other degradative pathways from the SCV in order to sustain the intracellular survival of *Salmonella* in this organism. The absence of effectors SopB or SifA results in the generation of a vacuolar compartment destined for degradation

generalised transduction using phage P22 HT105/1 *int*-201, as described (Maloy, 1990).

For complementation assays, genes *sopB* and *sifA* were PCR amplified from DNA obtained from the WT strain using primers flanking the promoter region and ORF of each gene (Table S14). PCR products were ligated to the pBAD-TOPO vector (Invitrogen) and transformed into chemically competent *E. coli* TOP10 cells (Invitrogen), according to the manufacturer instructions. Transformants were selected on LB agar containing Amp. Recombinant plasmids with either gene cloned in the same orientation as the $P_{ara\text{-}BAD}$ promoter were identified by PCR using combinations of primers listed in Table S14. Each plasmid was purified using the QIAPrep Spin Miniprep Kit (Qiagen) and transformed in the corresponding mutant strain for complementation assays. In addition, the WT and mutant strains containing the empty pBAD-TOPO vector were also generated as controls.

4.3 | *Dictyostelium* strains and growing conditions

D. discoideum strains AX2 (DBS0235519) (Ashworth & Watts, 1970) and AX2 VatM-GFP (DBS0235537) (Clarke et al., 2002) were obtained from Dicty Stock Center (Basu et al., 2013; Fey et al., 2013; Kreppel et al., 2004). Strains AX2 Atg9-GFP (Tung et al., 2010) and AX2 Atg16-GFP (Xiong et al., 2015) were kindly provided by Dr Ludwig Eichinger. All amoebae were cultured according to standard protocols (Fey et al., 2007). Amoebae were maintained at 23°C in SM agar (10 g/L tryptone, 1 g/L yeast extract, 1.08 g/L $MgSO_4$ x $7H_2O$, 1.9 g/L KH_2PO_4, 0.78 g/L K_2HPO_4 x $3H_2O$, 10 g/L glucose, 20 g/L agar agar) growing on top of a confluent lawn of *Klebsiella aerogenes* DBS0305928 until phagocytosis plaques were visible. Growing cells were transferred to liquid HL5 medium (14 g/L tryptone, 7 g/L yeast extract, 0.35 g/L Na_2HPO_4, 1.2 g/L KH_2PO_4, 15.2 g/L glucose) containing Amp (100 μg/mL) and streptomycin (Str; 300 μg/mL) and incubated at 23°C in tissue culture flasks when adherent cells were needed, or in glass flasks with agitation (180 rpm) when cells in suspension were needed. Cells were subcultured and used in the different assays when they reached 70–80% confluence in tissue culture flasks or when they reached exponential phase (1–2 × 10^6 cells/mL) when cultured in suspension. HL5 medium was supplemented with G418 (10 μg/mL) when growing the AX2 VatM-GFP strain and blasticidin S (5 μg/mL) when growing the AX2 Atg9-GFP and AX2 Atg16-GFP strains.

4.4 | Infection assays to detect SCVs by confocal microscopy

D. discoideum AX2 VatM-GFP grown in suspension axenically in HL5 medium was used. Amoebae were prepared by three cycles of centrifugation at 210*g* during 5 min at 4°C and resuspension in 1 ml of Soerensen buffer (2 g/L KH_2PO_4, 0.36 g/L Na_2HPO_4 x $2H_2O$, pH 6.0). Next, a suspension containing 1–2 × 10^6 amoeba/mL was prepared after counting viable cells in a Neubauer chamber. Bacteria transformed with plasmid pFCcGi, allowing constitutive expression of fluorescent protein mCherry (Figueira et al., 2013), were prepared from overnight (O/N) cultures by centrifuging at 3,420*g* during 5 min at 4°C and suspended in Soerensen buffer. Amoebae were infected in a final volume of 0.2 mL using a multiplicity of infection (MOI) of 100 bacteria/cell and incubated at 23°C during 1 hr without shaking to allow bacterial internalisation. Next, infected amoebae were centrifuged at 210*g* during 5 min at 4°C, and the pellet was washed three times in Soerensen buffer to eliminate extracellular bacteria. Finally, infected amoebae were suspended in 0.2 mL of Soerensen buffer and incubated at 23°C for up to 4.5 hr. Each sample was centrifuged at 210*g* during 5 min at 4°C, and the pellet was suspended in 40 μL of Soerensen buffer. All samples were individually mounted on a glass slide on top of a thin layer (100 μL) of 1% agarose in PBS. A coverslip

was placed over the sample and the borders sealed with colourless nail polish. Images were acquired with a Zeiss LSM 710 confocal microscope using the ZEN 2012 Back software (Zeiss). To detect the GFP label (amoebae), the sample was excited at 488 nm with an Argon laser, and the emitted fluorescence was detected with a 493–549 nm filter. To detect mCherry label (bacteria), the sample was excited at 543 nm with a HeNe laser, and fluorescence was detected with a 548–679 nm filter. All images were analysed and edited using FIJI software (Schindelin et al., 2012; Schneider et al., 2012).

4.5 | Infection assays to detect autophagy proteins associated with the SCV by confocal microscopy

D. discoideum strains AX2 Atg9-GFP and AX2 Atg16-GFP were grown axenically in HL5 medium to 80% confluence in T75 culture flasks. The day before an infection assay, 5×10^5 cells were seeded in a 35 mm ibidi μ-Dish (Cat. 81156) and incubated O/N at 23°C. On the day of the experiment, the cells were washed twice with 2 mL of Soerensen buffer. Amoebae were infected with WT *S.* Typhimurium transformed with plasmid pFCcGi in a final volume of 2 mL using a MOI of 100 bacteria/cell and incubated at 23°C during 1 hr without shaking to allow bacterial internalisation. Next, infected amoebae were washed three times in Soerensen buffer to eliminate extracellular bacteria, suspended in 2 mL of Soerensen buffer and incubated at 23°C for 3 hr. Images were acquired using a Nikon Ti eclipse spinning disk confocal microscope with a Nikon 60x/1.3 N.A. water objective and a CSU C910-50 camera and spinning head (Perkin Elmer) using Volocity software. All images were analysed and edited using FIJI software (Schindelin et al., 2012; Schneider et al., 2012).

4.6 | Infection assays to evaluate intracellular survival

The infection procedure was performed as indicated above. Next, infected amoebae were suspended in 1 mL of Soerensen buffer and incubated at 23°C for up to 6 hr. For each time point analysed, an aliquot was obtained and used to determine viable amoebae by Trypan staining and counting in a Neubauer chamber. Another aliquot was used to determine titers of intracellular bacteria. To do this, infected amoebae were washed once with Soerensen buffer supplemented with 10 μg/mL gentamicin, centrifuged at 210*g* during 5 min, washed with Soerensen buffer to remove the antibiotic and centrifuged at 210*g* during 5 min. Finally, the infected amoebae were lysed using 0.1% Triton X-100, serially diluted in PBS and plated on LB agar to determine CFU. The internalisation of each strain was calculated as intracellular CFU after the hour of internalisation (t = 0) divided by the inoculated CFU. The intracellular survival was calculated as the intracellular CFU at 3 and 6 hr post infection (t = 3 and t = 6, respectively) divided by the intracellular CFU at t = 0. Statistical significance was determined by a two-way ANOVA with Dunnett's test. All experiments were performed at least in biological triplicates.

4.7 | Subcellular fractionation and enrichment of SCVs from infected amoebae

Infected *D. discoideum* AX2 cells were used to obtain a fraction enriched in vacuolar compartments containing *S.* Typhimurium according to the protocol described in (Santos et al., 2015), with modifications. Amoebae grown in T225 tissue culture flasks in HL5 medium were washed three times with Soerensen buffer. Bacteria from late exponential phase cultures were collected by centrifugation at 3,420*g* during 5 min at 4°C and suspended in 50 mL of Soerensen buffer. Amoebae were infected using a MOI of 100 bacteria/cell and incubated at 23°C to allow bacterial internalisation. In the case of the WT strain, 1.2×10^8 amoebae were infected, while in the case of the Δ*sopB* and Δ*sifA* mutants, 2.4×10^8 amoebae were infected. Next, extracellular bacteria were removed by washing three times with Soerensen buffer. Finally, infected amoebae were maintained in Soerensen buffer and incubated during 3 hr at 23°C. After completion of the infection procedure, amoebae were washed three times with homogenization buffer (HB; 150 mM sucrose, 0.5 mM EGTA, 20 mM HEPES pH 7.4), scrapped from the tissue culture flask and suspended in 4 mL of HB supplemented with cOmplete Protease Inhibitor Cocktail (Roche) and 5 μg/mL cytochalasin D (Sigma-Aldrich) (HB complete), to decrease organelle clumping. Each cell suspension was then transferred to a Dounce homogeniser (Sigma-Aldrich) and lysed by stroking the pestle 35–40 times (1 stroke = 1 up +1 down) until more than 80% of free nuclei were visible under a light microscope. The homogenate was centrifuged at 100*g* during 5 min at 4°C to remove cell debris, the supernatant was collected and the pellet suspended in 1 mL of HB complete and centrifuged again. This procedure was repeated two times and the supernatants from the three centrifugations were combined (∼6 mL) and defined as PNS. In the case of the PNS from non-infected control, 1×10^8 CFU of the WT strain were added. Each PNS was loaded on top of a linear 10% (1.08 g/cm^3) to 25% (1.15 g/cm^3) OptiPrep gradient (Sigma-Aldrich) in HB with a 50% cushion prepared in 14 × 89 mm tubes (Beckman Coulter). Gradients were centrifuged at 210,000*g* during 3 hr at 4°C using an SW-41 swinging bucket rotor (Beckman) in an Optima L-100 XP Ultracentrifuge (Beckman Coulter) with low acceleration and no brake settings. After centrifugation, 12 fractions of 1 mL were collected from the top of the gradient. Each fraction was analysed by titrating the CFU via serial dilution and plating and by measuring the refraction index in a refractometer to determine its density.

4.8 | ELISA for *Salmonella* quantification

An anti-*Salmonella* ELISA developed to determine the presence of bacteria inside intact vacuoles was performed as described (Santos et al., 2015). A 96-well ELISA plate (Nunclon Immobilon) was coated with 70 μL of polyclonal rabbit anti-*Salmonella* antibody ab35156 (Abcam) suspended in PBS (5 μg/mL; 1:1,000) and incubated O/N at 4°C. The coated plate was blocked using 200 μL of blocking buffer (2% BSA from Sigma-Aldrich in PBS) during 1.5 hr at room

temperature. The plate was then washed four times with PBS, and the different samples were loaded. To quantify bacteria per fraction, a standard curve of serial two-fold dilutions of WT *S*. Typhimurium was prepared. For the fraction samples, an aliquot of 50 μL from F6 to F9 was diluted in 500 μL of HB (for pre-osmotic shock treatment) or in H_2O (for osmotic shock treatment). Next, each sample was loaded on different wells of the ELISA plate and incubated during 1 hr at room temperature. After that, the plate was washed with PBS and incubated O/N at 4°C with biotinylated rabbit anti-*Salmonella* antibody ab35156 (Abcam) diluted in blocking buffer (2 μg/mL; 1:2,000). Then, the plate was washed and incubated with Streptavidin-Peroxidase diluted in blocking buffer (Sigma-Aldrich, 1 mg/mL, 1:5,000) during 1 hr at room temperature. Subsequently, the plate was washed six times with PBS, the buffer was removed, 100 μL of SigmaFast OPD substrate solution (Sigma-Aldrich) was added, and the plate was incubated during 20–30 min at room temperature protected from light. The reaction was stopped by adding 50 μL of 10% SDS, and absorbance at 450 nm was determined in a FluoSTAR Omega microplate reader (BMG Labtech).

4.9 | Dot blot analysis of subcellular fractions

D. discoideum AX2 VatM-GFP cells were infected with WT *S*. Typhimurium and fractionated as described above. Each fraction was analysed by titrating the CFU via serial dilution and plating, and by measuring the refraction index in a refractometer to determine its density. Samples of each fraction (2 μL) were deposited on 0.2 μm pore-size nitrocellulose membranes (BioRad) and let to dry at room temperature. Blocking was performed by soaking the membranes in 5% BSA in TBS-T during 1 hr at room temperature. Next, membranes were incubated during 1 hr at room temperature with the corresponding primary antibodies diluted to 1:1,000 in 0.1% BSA in TBS-T. For *Salmonella* detection, a monoclonal mouse anti-*Salmonella* LPS was used (Abcam ab8272) and for GFP a polyclonal rabbit anti-GFP (Invitrogen A-6455) was used. Membranes were then washed three times with TBS-T and incubated during 30 min at room temperature with the corresponding secondary antibody conjugated with HRP, diluted to 1:5,000 in 0.1% BSA in TBS-T. Goat anti-rabbit IgG (BioRad 170–6515) and goat anti-mouse IgG (BioRad 170–6516) were used. Finally, membranes were washed three times with TBS-T and once with TBS, and incubated with SuperSignal West Femto maximum sensitivity substrate (Thermo Scientific) during 1 min. Images were captured using an Azure c400 imaging system.

4.10 | Protein precipitation and SDS-PAGE

Protein content in each fraction obtained was determined using the Micro BCA Protein Assay Kit (Thermo Fisher Scientific) according to the manufacturer instructions. Then, each sample was precipitated using the chloroform/methanol method (Wessel & Flügge, 1984). To do this, a volume of sample containing 20 μg of protein was mixed thoroughly with four volumes of methanol, and then one volume of chloroform was added and mixed. After that, three volumes of milliQ water were added, the mixture was thoroughly vortexed and then centrifuged at 16,100*g* during 10 min at 4°C. The organic layer was discarded and three volumes of methanol were added, mixed thoroughly and centrifuged as mentioned. Finally, the supernatant was discarded and the protein pellet was air-dried and stored frozen at −20°C. The protein pellets corresponding to F6 and F7 from each experiment and condition were combined in 30 μL of Laemmli sample buffer (Bio-Rad) and then heated at 95°C during 10 min. The samples were loaded in a NuPAGE 4–12% Bis-Tris pre-cast Gel (Invitrogen) and run at 200 V constant during 45 min. The gel was then fixed during 30 min in an aqueous solution containing 10% acetic acid and 40% ethanol. Proteins were stained by O/N incubation in colloidal Coomassie blue G-250 (8% ammonium sulfate, 0.8% phosphoric acid, 0.08% Coomassie blue G-250, 20% ethanol) and destained in milliQ water until bands were visible.

4.11 | Mass spectrometry sample preparation

Each gel lane corresponding to a sample was cut into 10 pieces and destained in 100 μL of a 1:1 mixture of acetonitrile and 0.2 M ammonium bicarbonate pH 8. Each gel piece was incubated at 30°C during 30 min with shaking. The liquid was discarded and the process repeated one more time. Then, cysteines were reduced by incubating with 10 mM DTT in 67 mM ammonium bicarbonate pH 8 at 56°C during 1 hr with shaking. The reduced cysteines were then alkylated using 55 mM iodoacetamide in 67 mM ammonium bicarbonate pH 8 and incubating at 25°C during 45 min with shaking. The gel pieces were then desiccated by adding 100% acetonitrile and incubating at 30°C during 30 min with shaking. In-gel protein digestion was performed by O/N incubation of the gel pieces with 1 μg of sequencing grade modified trypsin (Promega) in 67 mM ammonium bicarbonate pH 8 at 37°C. The next day, peptides from tryptic digestions were eluted from the gel pieces using a mixture containing 42.5% 50 mM ammonium bicarbonate, 42.5% acetonitrile and 5% formic acid and incubating at 30°C during 1 hr with shaking. Tryptic digestion samples were vacuum-dried and suspended in 2% acetonitrile, 0.1% formic acid in H_2O (solvent A) and sonicated during 10 min in a water bath. The samples were then desalted using Bond Elute OMIX C18 tip filters (Agilent) according to the manufacturer instructions, and the peptides were finally eluted in 50% acetonitrile, 1% formic acid in H_2O. These samples were vacuum-dried again and suspended in 10 μL of solvent A, sonicated during 10 min in a water bath. Finally, the peptide concentration of each sample was determined in a NanoDrop by measuring absorbance at 280 nm prior to its analysis by LC MS/MS.

4.12 | LC MS/MS data acquisition

Tryptic digests were analysed by nano-LC MS/MS. To do this, each sample was injected into a nano-HPLC system (EASY-nLC 1000,

Thermo Scientific) fitted with a reverse-phase column (Acclaim column, 15 cm × 50 μm ID, PepMap RSLC C18, 2 μm, 100 Å pore size, Thermo Scientific) equilibrated in solvent A. Peptides were separated at a flow rate of 300 nL/min using a linear gradient of 3–55% solvent B (80% acetonitrile, 0.08% formic acid) during 30 min. Peptide analysis was conducted in a Q-Exactive Plus mass spectrometer (Thermo-Scientific) set in data-dependent acquisition mode using a 30 s dynamic exclusion list. A resolution of 70,000 (at *m/z* 400) was used for MS scans. The 10 most intense ions were selected for HCD fragmentation and fragments were analysed in the Orbitrap.

4.13 | Proteomic data analysis

A target-decoy database including sequences from *Dictyostelium discoideum* (taxon identifier: 44689), *Salmonella enterica* subspecies *enterica* serovar Typhimurium strain 14028s (taxon identifier: 588858) downloaded from Uniprot consortium in March 2018, and 127 most common mass spectrometry contaminants was generated using PatternLab for Proteomics version 4.0 (Carvalho et al., 2016). For protein identification, the Comet search engine was set as follows: tryptic peptides; oxidation of methionine and carbamidomethylation as variable modifications, and 40 ppm of tolerance from the measured precursor *m/z*. XCorr and Z-Score were used as the primary and secondary search engine scores, respectively. Peptide spectrum matches were filtered using the Search Engine Processor (SEPro), and acceptable false discovery rate (FDR) criterion was set on 1% at the protein level. The Approximately Area Proportional Venn Diagram module was used to perform comparisons between conditions and to determine proteins uniquely identified in each situation. Proteins found in at least three biological replicates of one condition were considered as 'uniquely identified' when absent in all replicates of the other condition. For enrichment analysis, the TFold module was used to generate a volcano plot of the samples. This tool maximises the identifications of proteins differentially detected between two conditions that satisfies both a fold-change cutoff (that varies with the *t*-test *P*-value) and a stringency criterion that aims to detect proteins of low abundance under a Benjamini and Hochberg FDR estimator. For all comparisons, the FDR was fixed at 0.05. The TFold module then explored several values of the F-stringency parameter and selected the one that maximises the number of differentially detected proteins between the two datasets, for the specified *Q*-value of 0.05 (Carvalho et al., 2012a; Carvalho et al., 2012b). Functional clustering analyses were performed using DAVID bioinformatics resources (Huang et al., 2009a; Huang et al., 2009b).

ACKNOWLEDGMENTS

This work was supported by FONDECYT grants 1140754 and 1171844, to Carlos A. Santiviago. Camila Valenzuela and Ítalo M. Urrutia were supported by CONICYT fellowships 21140615 and 21150005, respectively. The team of Jost Enninga is supported by an ERC CoG grant (EndoSubvert), and acknowledges support from the ANR (StopBugEntry and AutoHostPath programs). Jost Enninga is a member of the LabExes IBEID and Milieu Interieur. The funders had no role in study design, data collection and interpretation, or the decision to submit the work for publication. We are indebted to Dr Ludwig Eichinger for kindly providing derivatives of *D. discoideum* AX2 expressing Atg9-GFP and Atg16-GFP used in this study. We thank Dr Macarena Varas and Carolina Hernández (Unidad de Microscopía Confocal, Facultad de Ciencias Químicas y Farmacéuticas, Universidad de Chile) for their technical assistance in microscopy experiments. We are grateful to Dr Magalie Duchateau and Dr Mariette Matondo (Mass Spectrometry for Biology-UTechS MSBio, Institut Pasteur) for their technical assistance in nano-LC MS/MS analyses. We thank the members of the Santiviago and Enninga teams for helpful feedback and discussion.

CONFLICT OF INTEREST

The authors declare that the research was conducted in the absence of any commercial or financial relationships that could be construed as a potential conflict of interest.

AUTHORS' CONTRIBUTION

Camila Valenzuela: Conceptualization, methodology, resources, investigation, formal analysis, project administration, funding acquisition, visualisation, writing-original draft preparation, writing-review and editing. **Magdalena Gil**: Conceptualization, methodology, resources, investigation, formal analysis, project administration, visualisation, writing-original draft preparation, writing-review and editing. **Ítalo M. Urrutia**: Methodology, investigation, writing-review and editing. **Andrea Sabag**: Methodology, investigation, project administration, writing-review and editing. **Jost Enninga**: Conceptualization, methodology, resources, supervision, visualisation, writing-original draft preparation, writing-review and editing. **Carlos A. Santiviago**: Conceptualization, methodology, resources, supervision, project administration, funding acquisition, writing-original draft preparation, writing-review and editing. Camila Valenzuela and Magdalena Gil contributed equally. All authors read and approved the final manuscript.

DATA AVAILABILITY STATEMENT

The mass spectrometry proteomics data that support the findings of this study are openly available in the ProteomeXchange Consortium via the PRIDE (Perez-Riverol et al., 2019) partner repository at https://www.ebi.ac.uk/pride/, reference number PXD014955.

ORCID

Camila Valenzuela https://orcid.org/0000-0002-5642-6188
Magdalena Gil https://orcid.org/0000-0002-9039-014X
Ítalo M. Urrutia https://orcid.org/0000-0002-5825-6901
Andrea Sabag https://orcid.org/0000-0003-3298-7287
Jost Enninga https://orcid.org/0000-0002-5218-349X
Carlos A. Santiviago https://orcid.org/0000-0002-7043-7908

REFERENCES

Adessi, C., Chapel, A., Vincon, M., Rabilloud, T., Klein, G., Satre, M., & Garin, J. (1995). Identification of major proteins associated with

Dictyostelium discoideum endocytic vesicles. *Journal of Cell Science*, *108*, 3331–3337.

Ashworth, J. M., & Watts, D. J. (1970). Metabolism of the cellular slime mould *Dictyostelium discoideum* grown in axenic culture. *The Biochemical Journal*, *119*, 175–182.

Basu, S., Fey, P., Pandit, Y., Dodson, R., Kibbe, W. A., & Chisholm, R. L. (2013). dictyBase 2013: Integrating multiple Dictyostelid species. *Nucleic Acids Research*, *41*, D676–D683.

Bleasdale, B., Lott, P. J., Jagannathan, A., Stevens, M. P., Birtles, R. J., & Wigley, P. (2009). The *Salmonella* pathogenicity Island 2-encoded type III secretion system is essential for the survival of *Salmonella enterica* serovar Typhimurium in free-living amoebae. *Applied and Environmental Microbiology*, *75*, 1793–1795.

Brandl, M. T., Rosenthal, B. M., Haxo, A. F., & Berk, S. G. (2005). Enhanced survival of *Salmonella enterica* in vesicles released by a soilborne *Tetrahymena* species. *Applied and Environmental Microbiology*, *71*, 1562–1569.

Brumell, J. H., Tang, P., Zaharik, M. L., & Finlay, B. B. (2002). Disruption of the *Salmonella*-containing vacuole leads to increased replication of *Salmonella enterica* serovar Typhimurium in the cytosol of epithelial cells. *Infection and Immunity*, *70*, 3264–3270.

Calvo-Garrido, J., Carilla-Latorre, S., Kubohara, Y., Santos-Rodrigo, N., Mesquita, A., Soldati, T., … Escalante, R. (2010). Autophagy in *Dictyostelium*: Genes and pathways, cell death and infection. *Autophagy*, *6*, 686–701.

Cardenal-Muñoz, E., Arafah, S., López-Jiménez, A. T., Kicka, S., Falaise, A., Bach, F., … Soldati, T. (2017). *Mycobacterium marinum* antagonistically induces an autophagic response while repressing the autophagic flux in a TORC1- and ESX-1-dependent manner. *PLoS Pathogens*, *13*, e1006344.

Carvalho, P. C., Fischer, J. S. G., Xu, T., Yates, J. R., & Barbosa, V. C. (2012). PatternLab: From mass spectra to label-free differential shotgun proteomics. *Current Protocols in Bioinformatics*, *40*, 13.19.1–13.19.18.

Carvalho, P. C., Lima, D. B., Leprevost, F. V., Santos, M. D. M., Fischer, J. S. G., Aquino, P. F., … Barbosa, V. C. (2016). Integrated analysis of shotgun proteomic data with PatternLab for proteomics 4.0. *Nature Protocols*, *11*, 102–117.

Carvalho, P. C., Yates, J. R., & Barbosa, V. C. (2012). Improving the TFold test for differential shotgun proteomics. *Bioinformatics*, *28*, 1652–1654.

Cirillo, D. M., Valdivia, R. H., Monack, D. M., & Falkow, S. (1998). Macrophage-dependent induction of the *Salmonella* pathogenicity Island 2 type III secretion system and its role in intracellular survival. *Molecular Microbiology*, *30*, 175–188.

Clarke, M., Köhler, J., Arana, Q., Liu, T., Heuser, J., & Gerisch, G. (2002). Dynamics of the vacuolar H^+-ATPase in the contractile vacuole complex and the endosomal pathway of *Dictyostelium* cells. *Journal of Cell Science*, *115*, 2893–2905.

Datsenko, K. A., & Wanner, B. L. (2000). One-step inactivation of chromosomal genes in *Escherichia coli* K-12 using PCR products. *Proceedings of the National Academy of Sciences of the United States of America*, *97*, 6640–6645.

Diacovich, L., Dumont, A., Lafitte, D., Soprano, E., Guilhon, A.-A., Bignon, C., … Méresse, S. (2009). Interaction between the SifA virulence factor and its host target SKIP is essential for *Salmonella* pathogenesis. *The Journal of Biological Chemistry*, *284*, 33151–33160.

Drecktrah, D., Knodler, L. A., Howe, D., & Steele-Mortimer, O. (2007). *Salmonella* trafficking is defined by continuous dynamic interactions with the endolysosomal system. *Traffic*, *8*, 212–225.

Dumont, A., Boucrot, E., Drevensek, S., Daire, V., Gorvel, J.-P., Poüs, C., … Méresse, S. (2010). SKIP, the host target of the *Salmonella* virulence factor SifA, promotes kinesin-1-dependent vacuolar membrane exchanges. *Traffic*, *11*, 899–911.

Dunn, J. D., Bosmani, C., Barisch, C., Raykov, L., Lefrançois, L. H., Cardenal-Muñoz, E., … Soldati, T. (2018). Eat prey, live: *Dictyostelium discoideum* as a model for cell-autonomous defenses. *Frontiers in Immunology*, *8*, 1906.

Feng, Y., Hsiao, Y.-H., Chen, H.-L., Chu, C., Tang, P., & Chiu, C.-H. (2009). Apoptosis-like cell death induced by *Salmonella* in *Acanthamoeba rhysodes*. *Genomics*, *94*, 132–137.

Fey, P., Dodson, R. J., Basu, S., & Chisholm, R. L. (2013). One stop shop for everything *Dictyostelium*: dictyBase and the Dicty stock center in 2012. In L. Eichinger & F. Rivero (Eds.), *Dictyostelium discoideum protocols* (pp. 59–92). Totowa, NJ: Humana Press.

Fey, P., Kowal, A. S., Gaudet, P., Pilcher, K. E., & Chisholm, R. L. (2007). Protocols for growth and development of *Dictyostelium discoideum*. *Nature Protocols*, *2*, 1307–1316.

Fields, P. I., Swanson, R. V., Haidaris, C. G., & Heffron, F. (1986). Mutants of *Salmonella typhimurium* that cannot survive within the macrophage are avirulent. *Proceedings of the National Academy of Sciences of the United States of America*, *83*, 5189–5193.

Figueira, R., Watson, K. G., Holden, D. W., & Helaine, S. (2013). Identification of *Salmonella* pathogenicity Island-2 type III secretion system effectors involved in intramacrophage replication of *S. enterica* serovar Typhimurium: Implications for rational vaccine design. *mBio*, *4*, e00065.

Frederiksen, R. F., & Leisner, J. J. (2015). Effects of *Listeria monocytogenes* EGD-e and *Salmonella enterica* ser. Typhimurium LT2 chitinases on intracellular survival in *Dictyostelium discoideum* and mammalian cell lines. *FEMS microbiology letters*, *362*, fnv067.

Fredlund, J., Santos, J. C., Stévenin, V., Weiner, A., Latour-Lambert, P., Rechav, K., … Enninga, J. (2018). The entry of *Salmonella* in a distinct tight compartment revealed at high temporal and ultrastructural resolution. *Cellular Microbiology*, *20*, e12816.

Gao, L. Y., Harb, O. S., & Kwaik, Y. A. (1997). Utilization of similar mechanisms by *Legionella pneumophila* to parasitize two evolutionarily distant host cells, mammalian macrophages and protozoa. *Infection and Immunity*, *65*, 4738–4746.

Garcia-del Portillo, F., & Finlay, B. B. (1995). Targeting of *Salmonella typhimurium* to vesicles containing lysosomal membrane glycoproteins bypasses compartments with mannose 6-phosphate receptors. *The Journal of Cell Biology*, *129*, 81–97.

Gaze, W. H., Burroughs, N., Gallagher, M. P., & Wellington, E. M. H. (2003). Interactions between *Salmonella typhimurium* and *Acanthamoeba polyphaga*, and observation of a new mode of intracellular growth within contractile vacuoles. *Microbial Ecology*, *46*, 358–369.

Hardt, W.-D., Chen, L.-M., Schuebel, K. E., Bustelo, X. R., & Galán, J. E. (1998). *S. typhimurium* encodes an activator of rho GTPases that induces membrane ruffling and nuclear responses in host cells. *Cell*, *93*, 815–826.

Hensel, M., Shea, J. E., Bäumler, A. J., Gleeson, C., Blattner, F., & Holden, D. W. (1997). Analysis of the boundaries of *Salmonella* pathogenicity Island 2 and the corresponding chromosomal region of *Escherichia coli* K-12. *Journal of Bacteriology*, *179*, 1105–1111.

Hernandez, L. D., Hueffer, K., Wenk, M. R., & Galán, J. E. (2004). *Salmonella* modulates vesicular traffic by altering phosphoinositide metabolism. *Science*, *304*, 1805–1807.

Heuser, J., Zhu, Q., & Clarke, M. (1993). Proton pumps populate the contractile vacuoles of *Dictyostelium* amoebae. *The Journal of Cell Biology*, *121*, 1311–1327.

Hoffmann, C., Finsel, I., Otto, A., Pfaffinger, G., Rothmeier, E., Hecker, M., … Hilbi, H. (2014). Functional analysis of novel Rab GTPases identified in the proteome of purified *Legionella*-containing vacuoles from macrophages. *Cellular Microbiology*, *16*, 1034–1052.

Holden, D. W., Salcedo, S. P., & Beuzón, C. R. (2002). Growth and killing of a *Salmonella enterica* serovar Typhimurium *sifA* mutant strain in the cytosol of different host cell lines. *Microbiology*, *148*, 2705–2715.

Huang, D. W., Sherman, B. T., & Lempicki, R. A. (2009a). Systematic and integrative analysis of large gene lists using DAVID bioinformatics resources. *Nature Protocols*, *4*, 44–57.

Huang, D. W., Sherman, B. T., & Lempicki, R. A. (2009b). Bioinformatics enrichment tools: Paths toward the comprehensive functional analysis of large gene lists. *Nucleic Acids Research*, *37*, 1–13.

Jia, K., Thomas, C., Akbar, M., Sun, Q., Adams-Huet, B., Gilpin, C., & Levine, B. (2009). Autophagy genes protect against *Salmonella typhimurium* infection and mediate insulin signaling-regulated pathogen resistance. *Proceedings of the National Academy of Sciences of the United States of America*, *106*, 14564–14569.

Knuff, K., & Finlay, B. B. (2017). What the SIF is happening–The role of intracellular *Salmonella*-induced filaments. *Frontiers in Cellular and Infection Microbiology*, *7*, 335.

Koliwer-Brandl, H., Knobloch, P., Barisch, C., Welin, A., Hanna, N., Soldati, T., & Hilbi, H. (2019). Distinct *Mycobacterium marinum* phosphatases determine pathogen vacuole phosphoinositide pattern, phagosome maturation, and escape to the cytosol. *Cellular Microbiology*, *21*, e13008.

Kreibich, S., Emmenlauer, M., Fredlund, J., Rämö, P., Münz, C., Dehio, C., … Hardt, W. D. (2015). Autophagy proteins promote repair of endosomal membranes damaged by the *Salmonella* type three secretion system 1. *Cell Host & Microbe*, *18*, 527–537.

Kreppel, L., Fey, P., Gaudet, P., Just, E., Kibbe, W. A., Chisholm, R. L., & Kimmel, A. R. (2004). dictyBase: A new *Dictyostelium discoideum* genome database. *Nucleic Acids Research*, *32*, D332–D333.

Mallo, G. V., Espina, M., Smith, A. C., Terebiznik, M. R., Alemán, A., Finlay, B. B., … Brumell, J. H. (2008). SopB promotes phosphatidylinositol 3-phosphate formation on *Salmonella* vacuoles by recruiting Rab5 and Vps34. *The Journal of Cell Biology*, *182*, 741–752.

Maloy, S. (1990). *Experimental techniques in bacterial genetics*. Boston, MA: Jones and Bartlett Publishers.

Maskell, D., & Mastroeni, P. (2006). *Salmonella infections: Clinical, immunological and molecular aspects*. Cambridge, UK: Cambridge University Press.

Méresse, S., Steele-Mortimer, O., Finlay, B. B., & Gorvel, J.-P. (1999). The rab7 GTPase controls the maturation of *Salmonella typhimurium*-containing vacuoles in HeLa cells. *The EMBO Journal*, *18*, 4394–4403.

Müller-Taubenberger, A., Kortholt, A., & Eichinger, L. (2013). Simple system–Substantial share: The use of *Dictyostelium* in cell biology and molecular medicine. *European Journal of Cell Biology*, *92*, 45–53.

Oh, Y. K., Alpuche-Aranda, C., Berthiaume, E., Jinks, T., Miller, S. I., & Swanson, J. A. (1996). Rapid and complete fusion of macrophage lysosomes with phagosomes containing *Salmonella typhimurium*. *Infection and Immunity*, *64*, 3877–3883.

Ohlson, M. B., Huang, Z., Alto, N. M., Blanc, M.-P., Dixon, J. E., Chai, J., & Miller, S. I. (2008). Structure and function of *Salmonella* SifA indicate that its interactions with SKIP, SseJ, and RhoA family GTPases induce endosomal tubulation. *Cell Host & Microbe*, *4*, 434–446.

Patel, J. C., & Galán, J. E. (2006). Differential activation and function of rho GTPases during *Salmonella*–host cell interactions. *The Journal of Cell Biology*, *175*, 453–463.

Peracino, B., Balest, A., & Bozzaro, S. (2010). Phosphoinositides differentially regulate bacterial uptake and Nramp1-induced resistance to *Legionella* infection in *Dictyostelium*. *Journal of Cell Science*, *123*, 4039–4051.

Perez-Riverol, Y., Csordas, A., Bai, J., Bernal-Llinares, M., Hewapathirana, S., Kundu, D. J., … Vizcaíno, J. A. (2019). The PRIDE database and related tools and resources in 2019: Improving support for quantification data. *Nucleic Acids Research*, *47*, D442–D450.

Ramos-Morales, F. (2012). Impact of *Salmonella enterica* type III secretion system effectors on the eukaryotic host cell. *ISNR Cell Biology*, *2012*, 787934.

Rappl, C., Deiwick, J., & Hensel, M. (2003). Acidic pH is required for the functional assembly of the type III secretion system encoded by *Salmonella* pathogenicity Island 2. *FEMS Microbiology Letters*, *226*, 363–372.

Rehfuss, M. Y. M., Parker, C. T., & Brandl, M. T. (2011). *Salmonella* transcriptional signature in *Tetrahymena* phagosomes and role of acid tolerance in passage through the protist. *The ISME Journal*, *5*, 262–273.

Riquelme, S., Varas, M., Valenzuela, C., Velozo, P., Chahin, N., Aguilera, P., … Santiviago, C. A. (2016). Relevant genes linked to virulence are required for *Salmonella* Typhimurium to survive intracellularly in the social amoeba *Dictyostelium discoideum*. *Frontiers in Microbiology*, *7*, 1305.

Rosel, D., & Kimmel, A. R. (2006). The COP9 signalosome regulates cell proliferation of *Dictyostelium discoideum*. *European Journal of Cell Biology*, *85*, 1023–1034.

Santiviago, C. A., Reynolds, M. M., Porwollik, S., Choi, S.-H., Long, F., Andrews-Polymenis, H. L., & McClelland, M. (2009). Analysis of pools of targeted *Salmonella* deletion mutants identifies novel genes affecting fitness during competitive infection in mice. *PLoS Pathogens*, *5*, e1000477.

Santos, J. C., Duchateau, M., Fredlund, J., Weiner, A., Mallet, A., Schmitt, C., … Enninga, J. (2015). The COPII complex and lysosomal VAMP7 determine intracellular *Salmonella* localization and growth. *Cellular Microbiology*, *17*, 1699–1720.

Schindelin, J., Arganda-Carreras, I., Frise, E., Kaynig, V., Longair, M., Pietzsch, T., … Cardona, A. (2012). Fiji: An open-source platform for biological-image analysis. *Nature Methods*, *9*, 676–682.

Schneider, C. A., Rasband, W. S., & Eliceiri, K. W. (2012). NIH image to ImageJ: 25 years of image analysis. *Nature Methods*, *9*, 671–675.

Segal, G., & Shuman, H. A. (1999). *Legionella pneumophila* utilizes the same genes to multiply within *Acanthamoeba castellanii* and human macrophages. *Infection and Immunity*, *67*, 2117–2124.

Sillo, A., Matthias, J., Konertz, R., Bozzaro, S., & Eichinger, L. (2011). *Salmonella typhimurium* is pathogenic for *Dictyostelium* cells and subverts the starvation response. *Cellular Microbiology*, *13*, 1793–1811.

Singh, V., Schwerk, P., & Tedin, K. (2018). Rapid isolation of intact *Salmonella*-containing vacuoles using paramagnetic nanoparticles. *Gut Pathogens*, *10*, 33.

Skriwan, C., Fajardo, M., Hägele, S., Horn, M., Wagner, M., Michel, R., … Steinert, M. (2002). Various bacterial pathogens and symbionts infect the amoeba *Dictyostelium discoideum*. *International Journal of Medical Microbiology*, *291*, 615–624.

Stanley, R., Ragusa, M., & Hurley, J. (2014). The beginning of the end: How scaffolds nucleate autophagosome biogenesis. *Trends in Cell Biology*, *24*, 73–81.

Steele-Mortimer, O. (2008). The *Salmonella*-containing vacuole–Moving with the times. *Current Opinion in Microbiology*, *11*, 38–45.

Steele-Mortimer, O., Méresse, S., Gorvel, J.-P., Toh, B.-H., & Finlay, B. B. (1999). Biogenesis of *Salmonella typhimurium*-containing vacuoles in epithelial cells involves interactions with the early endocytic pathway. *Cellular Microbiology*, *1*, 33–49.

Steiner, B., Weber, S., & Hilbi, H. (2018). Formation of the *Legionella*-containing vacuole: Phosphoinositide conversion, GTPase modulation and ER dynamics. *International Journal of Medical Microbiology*, *308*, 49–57.

Stévenin, V., Chang, Y.-Y., Le Toquin, Y., Duchateau, M., Gianetto, Q. G., Luk, C. H., … Enninga, J. (2019). Dynamic growth and shrinkage of the *Salmonella*-containing vacuole determines the intracellular pathogen niche. *Cell Reports*, *29*, 3958–3973.

Swart, A. L., Harrison, C. F., Eichinger, L., Steinert, M., & Hilbi, H. (2018). *Acanthamoeba* and *Dictyostelium* as cellular models for *Legionella* infection. *Frontiers in Cellular and Infection Microbiology*, *8*, 61.

Taylor-Mulneix, D. L., Hamidou Soumana, I., Linz, B., & Harvill, E. T. (2017). Evolution of Bordetellae from environmental microbes to human respiratory pathogens: Amoebae as a missing link. *Frontiers in Cellular and Infection Microbiology*, *7*, 510.

Tezcan-Merdol, D., Ljungström, M., Winiecka-Krusnell, J., Linder, E., Engstrand, L., & Rhen, M. (2004). Uptake and replication of *Salmonella enterica* in *Acanthamoeba rhysodes*. *Applied and Environmental Microbiology*, *70*, 3706–3714.

Thurston, T. L. M., Ryzhakov, G., Bloor, S., von Muhlinen, N., & Randow, F. (2009). The TBK1 adaptor and autophagy receptor NDP52 restricts the proliferation of ubiquitin-coated bacteria. *Nature Immunology*, *10*, 1215–1221.

Thurston, T. L. M., Wandel, M. P., von Muhlinen, N., Foeglein, Á., & Randow, F. (2012). Galectin 8 targets damaged vesicles for autophagy to defend cells against bacterial invasion. *Nature*, *482*, 414–418.

Tung, S. M., Ünal, C., Ley, A., Peña, C., Tunggal, B., Noegel, A. A., … Eichinger, L. (2010). Loss of *Dictyostelium* ATG9 results in a pleiotropic phenotype affecting growth, development, phagocytosis and clearance and replication of *Legionella pneumophila*. *Cellular Microbiology*, *12*, 765–780.

Urrutia, Í. M., Sabag, A., Valenzuela, C., Labra, B., Álvarez, S. A., & Santiviago, C. A. (2018). Contribution of the twin-arginine translocation system to the intracellular survival of *Salmonella* Typhimurium in *Dictyostelium discoideum*. *Frontiers in Microbiology*, *9*, 3001.

Urwyler, S., Nyfeler, Y., Ragaz, C., Lee, H., Mueller, L. N., Aebersold, R., & Hilbi, H. (2009). Proteome analysis of *Legionella* vacuoles purified by magnetic immunoseparation reveals secretory and endosomal GTPases. *Traffic*, *10*, 76–87.

Varas, M. A., Riquelme-Barrios, S., Valenzuela, C., Marcoleta, A. E., Berríos-Pastén, C., Santiviago, C. A., & Chávez, F. P. (2018). Inorganic polyphosphate is essential for *Salmonella* Typhimurium virulence and survival in *Dictyostelium discoideum*. *Frontiers in Cellular and Infection Microbiology*, *8*, 8.

Waterman, S. R., & Holden, D. W. (2003). Functions and effectors of the *Salmonella* pathogenicity Island 2 type III secretion system. *Cellular Microbiology*, *5*, 501–511.

Weber, S., Steiner, B., Welin, A., & Hilbi, H. (2018). *Legionella*-containing vacuoles capture PtdIns(4)P-rich vesicles derived from the Golgi apparatus. *mBio*, *9*, e02420.

Wei, N., Serino, G., & Deng, X.-W. (2008). The COP9 signalosome: More than a protease. *Trends in Biochemical Sciences*, *33*, 592–600.

Wessel, D., & Flügge, U. I. (1984). A method for the quantitative recovery of protein in dilute solution in the presence of detergents and lipids. *Analytical Biochemistry*, *138*, 141–143.

Wildschutte, H., & Lawrence, J. G. (2007). Differential *Salmonella* survival against communities of intestinal amoebae. *Microbiology*, *153*, 1781–1789.

Wildschutte, H., Wolfe, D. M., Tamewitz, A., & Lawrence, J. G. (2004). Protozoan predation, diversifying selection, and the evolution of antigenic diversity in *Salmonella*. *Proceedings of the National Academy of Sciences of the United States of America*, *101*, 10644–10649.

World Health Organization. (2015). *WHO estimates of the global burden of foodborne diseases*. Geneva, Switzerland: World Health Organization.

Xiong, Q., Ünal, C., Matthias, J., Steinert, M., & Eichinger, L. (2015). The phenotypes of ATG9, ATG16 and ATG9/16 knock-out mutants imply autophagy-dependent and -independent functions. *Open Biology*, *5*, 150008.

Yu, H. B., Croxen, M. A., Marchiando, A. M., Ferreira, R. B. R., Cadwell, K., Foster, L. J., & Finlay, B. B. (2014). Autophagy facilitates *Salmonella* replication in HeLa cells. *mBio*, *5*, e00865.

Zheng, Y. T., Shahnazari, S., Brech, A., Lamark, T., Johansen, T., & Brumell, J. H. (2009). The adaptor protein p62/SQSTM1 targets invading bacteria to the autophagy pathway. *Journal of Immunology*, *183*, 5909–5916.

SUPPORTING INFORMATION

Additional supporting information may be found online in the Supporting Information section at the end of this article.

How to cite this article: Valenzuela C, Gil M, Urrutia ÍM, Sabag A, Enninga J, Santiviago CA. SopB- and SifA-dependent shaping of the *Salmonella*-containing vacuole proteome in the social amoeba *Dictyostelium discoideum*. *Cellular Microbiology*. 2021;23:e13263. https://doi.org/10.1111/cmi.13263